

DEVELOPMENT AND VERIFICATION OF DYNAMIC
THERMAL MODELS FOR FLUID
POWER COMPONENTS AND
SYSTEMS

By

DENNIS GARY MILLER

//

Bachelor of Science

Oklahoma State University

Stillwater, Oklahoma

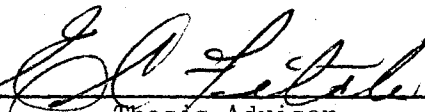
1972

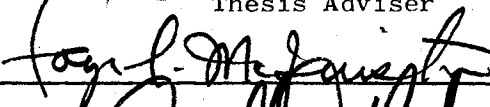
Submitted to the Faculty of the Graduate College
of the Oklahoma State University
in partial fulfillment of the requirements
for the Degree of
MASTER OF SCIENCE
December, 1974


MAR 28 1975

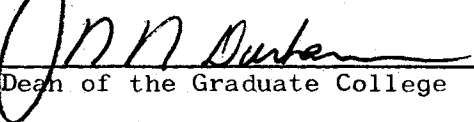
DEVELOPMENT AND VERIFICATION OF DYNAMIC
THERMAL MODELS FOR FLUID
POWER COMPONENTS AND
SYSTEMS

Thesis Approved:



Thesis Adviser






Dean of the Graduate College

903405

ACKNOWLEDGMENTS

I would like to give my special thanks to Dr. E. C. Fitch for his enthusiastic interest and encouragement during my graduate study.

Dr. J. D. Parker and Dr. F. C. McQuiston offered many helpful comments and suggestions for improving the quality of the final manuscript. I wish to express my gratitude to them for their criticisms and their interest in me personally.

The Fluid Power Research Center and the U. S. Army Mobility Equipment Research and Development Center, Ft. Belvoir, Virginia, deserve recognition for sponsoring the investigations of this report and for extending financial support.

My associates at the Fluid Power Research Center have been invaluable throughout the course of this study. I wish to thank all of them, in particular, S. K. R. Iyengar for his assistance in developing the various models, and B. Koger, who aided me throughout the experimental testing program.

I am thankful to Miss Carol Armour, Miss Velda Davis, and Mrs. Marilyn Bond for typing the several rough drafts and the final manuscript.

To my parents I express my sincere appreciation and thanks for their encouragement and support.

TABLE OF CONTENTS

Chapter	Page
I. INTRODUCTION	1
II. PREVIOUS INVESTIGATION	5
III. DEVELOPMENT OF STEADY-STATE AND DYNAMIC COMPONENT MODELS	10
Heat Exchangers	11
Reservoir	18
9 Fluid Power Pump	22
IV. DEVELOPMENT OF STEADY-STATE AND DYNAMIC MODELS FOR COMPLETE SYSTEMS	27
Total System Without Heat Exchangers	27
Total System With a Liquid-to-Air Heat Exchanger	35
V. EXPERIMENTAL VERIFICATION	41
Component Testing	42
Total System Testing	56
VI. CONCLUSIONS AND RECOMMENDATIONS	73
Recommendations for Further Study	75
SELECTED BIBLIOGRAPHY	77
APPENDIX A - LARGE SCALE SYSTEM CONSIDERATION OF A TOTAL SYSTEM MODEL	80
APPENDIX B - INSTRUMENTATION	85

LIST OF TABLES

Table	Page
I. Summary of Steady-State Tests for a Liquid-to-Air Heat Exchanger	43
II. Error Summary for Liquid-to-Air Heat Exchanger Simulations	46
III. Summary of Steady-State Tests for a Liquid-to-Liquid Heat Exchanger	49
IV. Error Between Experimental and Predicted Results for the Liquid-to-Liquid Heat Exchanger	51
V. Summary of Steady-State Tests for an Open-Center System Without Heat Exchanger	59
VI. Error Summary of Simulations for Open-Center System Without Heat Exchanger	61
VII. Error Summary of Computed and Experimental Values for the System With a Liquid-to-Air Heat Exchanger	70

LIST OF FIGURES

Figure	Page
1. Representation of (a) A Liquid-to-Air Heat Exchanger, (b) A Liquid-to-Liquid Heat Exchanger	13
2. Representation of a Reservoir	20
3. Schematic of an Open-Center System Without a Heat Exchanger	28
4. Wheatstone Bridge Analogy of an Open-Center Directional Control Valve	31
5. Open-Center System With a Liquid-to-Air Heat Exchanger	36
6. Liquid-to-Air Heat Exchanger Response to Increasing Inlet Fluid Temperature	47
7. Typical Results for an Increase of Inlet Fluid Temperature	52
8. Typical Results for a Decrease of Inlet Fluid Temperature	53
9. Effects of a Dynamic Change in Coolant Flow Rate Through the Heat Exchanger	54
10. Scotch Yoke Mechanism	57
11. Flowchart for Thermal Analysis of an Open-Center System Without Heat Exchangers	62
12. Test Results Versus Computed Values for an Open-System Without Heat Exchangers	63
13. Cyclic Operation of an Open-Center System: (a) Spool Displacement, (b) System Pressure, (c) Pressure at Port A of Control Valve, (d) Pressure at Port B of Control Valve	65
14. Test Results for Duty Cycle Operation of the System Without Heat Exchangers	66
15. Test Results for a Constant System Load	67

Figure	Page
16. Test Results for an Open-Center System With a Liquid-to-Air Heat Exchanger	69
17. Cyclic Test Results for an Open-Center System With a Liquid-to-Air Heat Exchanger ($Q_f = 50$ lpm)	71
18. Voltage-Current Characteristic of Platinum Resistance Temperature Sensor	88

NOMENCLATURE

Notation

A	Heat transfer area, sq. ft.
C _{eq}	Equivalent thermal capacitance, Btu/°F
C _p	Specific heat, Btu/lb _m /°F
H _{in}	Rate of thermal energy entering a component, Btu/min.
H _{out}	Rate of thermal energy leaving a component, Btu/min.
H _{st}	Rate of thermal energy storage in a component, Btu/min.
H _{tr}	Rate of thermal energy transferred from a component, Btu/min.
k ₁	Constant for dimensional consistency, 0.000643 Btu/sec/in-lb _f -min.
k ₂	Constant for dimensional consistency, 0.0167 hr/min.
KE	Kinetic energy, Btu/min.
m	Mass, lb _m
\dot{m}	Mass flow rate, lb _m /min.
Q	Flow rate, gpm.
t	Time, min.
T _{amb}	Ambient temperature, °F
T _c	Coolant temperature, °F
T _f	Fluid temperature, °F
T _w	Wall temperature, °F
U	Overall heat transfer coefficient, Btu/hr/sq. ft./°F
V	Velocity, ft/sec.

Notation

W_{in}	Input work energy, Btu/min.
W_{out}	Output work energy, Btu/min.
ΔP	Differential pressure, psig
ΔT	Differential temperature, °F
η	Pump efficiency
ρ	Mass density, lb _m /gal.
ΣH_g	Total rate of heat addition, Btu/min.

Subscripts

A	Port A of open-center valve
Air	Air
B	Port B of open-center valve
C	Coolant
F	Fluid
i	inlet
H	Liquid-to-air heat exchanger
L	Liquid-to-liquid heat exchanger
o	Outlet
p	Pump
R	Reservoir
T	Tank
w	Wall
1	Orifice 1 of open-center valve
2	Orifice 2 of open-center valve
3	Orifice 3 of open-center valve
4	Orifice 4 of open-center valve
5	Orifice 5 of open-center valve

CHAPTER I

INTRODUCTION

Until recently, the design engineers of fluid power components and systems paid scant attention to thermal considerations of their products. Motivation to know more about thermal phenomena in hydraulic systems is a result of the desire for higher system operating pressures and efficiencies. It is known that higher system pressures bring with them increases in fluid temperatures. Systems with insufficient or inefficient cooling and operating at high pressure can subject circuits to high fluid temperatures. If a hydraulically powered machine continues to operate at high temperatures, a host of temperature-induced problems can arise. General system performance degrades; oil based fluids separate; there is a greater frequency of material failures; combustion and explosion possibilities are increased; and personal safety hazards are greatly amplified. These are a few problems that arise from using high powered, high pressure, and high temperature hydraulic systems. Thus, it can be seen that there is a necessity for system designers to have simple tools for accurately predicting temperatures in fluid power systems.

The fundamental systems theory concepts of lumped-parameter static and dynamic modeling are well suited for thermal analysis of fluid power components and systems. This, combined with the basic laws of heat transfer and thermodynamics, enables the derivation of thermal models for prediction of temperature as well as heat transfer. Neither of the above

concepts is new to the fluid power industry. Static or steady-state thermal analysis has been used to aid in sizing heat exchangers and other components. The basis for component sizing is that an operating system will reach steady-state conditions, and the fluid temperature is the average temperature at some point in the system. The reservoir is usually the point at which an average temperature measurement is made since the bulk of the fluid in most systems is held by the reservoir.

Steady-state analyses are useful in some parameter identification but cannot be used to determine component or system time constants. Nothing is learned about the transient response of a system to an input or set of inputs, and localized hot spots can go undetected. A mathematical model (lumped-parameter, distributed-parameter, finite difference, etc!) that can be solved and that provides the desired accuracy is obtained by applying engineering judgment to the component or system.

Hydraulic components and systems are distributed-parameter in nature and are most accurately modeled by nonlinear algebraic and/or high-ordered partial differential equations. The results provided by the solution of such equations are quite accurate but are often impossible to obtain due to a number of unknown parameters in the model. The purpose of this thesis is to present a general lumped-parameter modeling technique that is applicable to steady-state and dynamic thermal modeling of components as well as systems. Such models are obtained by "lumping" the thermal capacitance and conductance (reciprocal of resistance) of an element into distinct parameters and proceeding with the model development. Thus, the parameters involved are few and can be determined from steady-state and dynamic test data.

The approximations made by lumping parameters in a model for a

component or a system are shown to be good if there is reasonable agreement between experimental data and predicted results of the model. Better lumping is done by dividing the component or system into sections and formulating a model for each. The total model is then obtained by combining the models for each segment. All of the lumped-parameters in such models are difficult to obtain, and the models are generally of high-order. Consequently, it is desirable to combine elements into groups of components and to obtain a model for the group rather than to model each individually or in segments.

Examples of component lumped-parameter thermal modeling and system lumped-parameter thermal modeling are presented in the following pages.

The incorporation of a lumped-parameter component model into a complete system model is shown to be a problem of manipulation. Steady-state and dynamic test data are used for the identification of parameters for component and system models and are used in their verification.

The following chapter presents a brief survey of previous work in both steady-state and dynamic thermal analysis and modeling of hydraulic systems. Chapters III, IV, and V contain the major efforts of this thesis.

Chapter III presents the derivations of steady-state and dynamic lumped-parameter thermal models for several components and explains the conditions for which they are valid. The components that are modeled include liquid-to-air and liquid-to-liquid heat exchangers, a pump, and a reservoir cooled by natural convection. Total system steady-state and dynamic lumped-parameter thermal models with and without heat exchanger dynamics are presented in Chapter IV. Chapter V discusses the results of an experimental testing program for component and system model

verification. Parameters for component and system models are identified from steady-state and dynamic test data. A comparison is made of dynamic test data to the results of computer simulations of various models.

General conclusions and recommendations are made in Chapter VI. Appendix A gives a derivation to show that one of the total system models is less than second-order. This is not applicable to all systems, but it does apply to one of the systems considered in this study. Appendix B discusses the instrumentation that was used for experimental thermal analysis.

CHAPTER II

PREVIOUS INVESTIGATION

There exists a great deal of literature concerning steady-state and transient temperature analysis for a number of physical phenomena. However, if the field is limited to the subject of thermal analysis of fluid power systems, it is found that there is a small amount of literature available. To complicate the situation further, the majority of this information concerns itself with steady-state thermal analysis. Thus, published information on the subject of dynamic thermal analysis of hydraulic systems is scant indeed.

Perhaps the most encompassing work on thermal analysis of hydraulic components and systems has been done by Parker and McQuiston (27). This study is extensive and sufficiently general to be applicable to any component or system thermal analysis, but it is based on the steady energy equation. As a result, this report is relevant only for steady-state thermal analysis. However, due to its generality, it can be considered as a summary of the state of the art for steady-state thermal analysis of hydraulic components and systems.

Magnus presents an analysis similar to those of Parker and McQuiston (26) (27) along with some experimental results for pressure versus temperature characteristics of hydraulic fluid due to pumping. A steady-state analysis of the "727B" hydraulic system is done by Abiodun (1), who presents a computerized algorithm to predict steady-state component and

system temperatures. The computer program developed here uses lumped-parameter models but is highly specialized to treat only a specific system. Consequently, the program is inapplicable for any other analysis. Graphical methods for calculating steady-state system temperatures are shown by Wood (31) to provide rapid and reasonably accurate predictions of hydraulic system temperatures.

A technique for determining the steady-state efficiency of pumps or motors from temperature, pressure, and flow measurements is described by Stern (29). In addition to the measurements of these physical variables, the thermodynamic properties of the working fluid must also be known. The construction of an enthalpy-temperature (h-T) diagram for Mil-H-5606 hydraulic fluid from the Maxwell relations is presented. The method for constructing h-T diagrams for hydraulic fluids is applicable to all available fluids. The advantage of this technique is that knowing the inlet and outlet fluid pressures and temperatures gives the enthalpy and entropy increases in the fluid. A direct measurement of the input and output work of a pump or motor was obtained from the increases in enthalpy and entropy since the external surface of the pump was insulated to minimize heat transfer to the atmosphere. Thus, the steady-state efficiency of the test machine was determined independent of the shaft torque and speed characteristics, which are generally used for efficiency calculations.

Norgard (24) presents a discussion similar to Stern's and applies the method to a hydrostatic pump. Experimental data is given for this application. The attractiveness of the method presented by Stern and Norgard is that the power loss for any component can be determined. However, the major drawback of the method is that it is relevant only to components and systems which are operating at steady-state conditions.

Steady-state thermal analysis is important, but more significance should be given to dynamic thermal analysis. Mathakia (18) derives dynamic lumped-parameter models for predicting wall temperatures and outlet fluid temperatures of components based on a knowledge of inlet conditions and application of the unsteady energy equation. The methods that are presented show the existence of transient temperatures, but the procedure used for identifying the unknown heat transfer coefficients is not discussed. Ebbesen (7) gives a more recent summary of the state of the art in steady-state thermal modeling and advances a basic theory for dynamic modeling of components from applications of the unsteady energy equation. This work is left open for changes and further development. The same author presents an approach for identifying some parameters for dynamic thermal component models from steady-state test data (5). A lumped-parameter dynamic thermal model for a fluid power pump is also presented by Ebbesen (6). Basic mathematical modeling considerations are stated, and an experimental procedure is advanced for verifying the analytical model.

Heat exchangers are probably the most influential sources on transient and steady-state temperatures. Much work has been done in heat exchanger analysis for a variety of industrial uses. The techniques of heat exchanger analyses done outside of the hydraulic industry can be adapted and applied in the thermal analysis of fluid power systems.

Finlay and Smith (9) present a complex linear, distributed-parameter model for one side of a heat exchanger and demonstrate the effects of disturbances in flow rate through the exchanger. They also mention the concept of thermal capacitance, but no use is made of it mathematically. Gilles (12) uses an analogous approach to the above in developing a

thermal model for a heat exchanger. The linear, partial differential equation that is obtained is then solved by Laplace transforms.

Thal-Larsen and Loscutoff (30) deviate from the classical method of using distributed-parameter, partial differential equations to model heat exchangers and derive a linear, ordinary differential equation model. Simplification of a partial differential equation to an ordinary differential equation model is done by Stermole and Larson (28). This simplified model is verified by experimental data for a steam-water heat exchanger. Messa et al. (21) present a scalar pulse testing method to determine the frequency response of several heat exchanger configurations. The differential equation model used here was fitted to experimental data to give the dynamic response of the exchanger.

Computer simulation of a thermal model for a concentric tube heat exchanger was done by Wood and Sastry (32). A lumped-parameter model was obtained from the simplification of a distributed-parameter model, and it was numerically solved by a digital computer using finite difference techniques.

The exchanger models presented by the above mentioned authors are only a few of many that have been derived. The models cited here are representative of those commonly used for modeling the dynamic thermal behavior of heat exchangers.

The dynamic models presented in the articles discussed above are first or second-order, linear, ordinary differential equations or fourth-order, linear partial differential equations. The models are applicable to thermal analysis of fluid power systems provided that the heat transfer coefficients of the exchanger being studied are used in the equations of the model. The disadvantage of some of the models is

that they are too complex to use in constructing a dynamic thermal model for a system employing a heat exchanger.

From the foregoing discussion it is apparent that experimentally verified dynamic thermal models for components and systems have not yet been advanced by the hydraulic industry. The literature survey presented above exemplifies that most of the previous work in thermal analysis of fluid power machinery has been concerned with steady-state rather than dynamic analysis. Published literature on the subject of hydraulic system thermal analysis is not voluminous, and less information exists for dynamic thermal analysis of fluid power systems. Consequently, system analysts and designers have few usable tools for performing dynamic thermal analyses of hydraulic systems and are left with the recourse of inventing and developing methods which meet the demands of today's technology.

The following chapter presents the derivations of lumped-parameter steady-state and dynamic thermal models for several fluid power components.

CHAPTER III

DEVELOPMENT OF STEADY-STATE AND DYNAMIC COMPONENT MODELS

The lumped-parameter modeling concept is an ideal basis for the development of steady-state and dynamic thermal models for fluid power components and systems. Since hydraulic components are distributed-parameter in nature, considerable mathematical simplicity is achieved with lumped-parameter models. Only the inputs, outputs, and initial conditions need to be considered in a mathematical model. The resultant equations which constitute the component or system model are in a form suitable for digital or analog computer simulation. Disadvantages of lumped-parameter models are that they are less accurate than distributed-parameter models due to the "lumping" of parameters, and at higher frequencies such models often break down (34). Lumped-parameter thermal models for the hydraulic components and systems studied in this investigation are considered to be sufficiently accurate since rapid transients and high frequency inputs will not be encountered.

It is assumed that the thermal capacitance and thermal conductance of components or systems can be lumped into distinct parameters. In this chapter, steady-state and dynamic thermal models are derived from this basis for the components which, when used in a system, dominate the dynamic thermal behavior of any hydraulically powered machine. The

components that are modeled include heat exchangers, a reservoir, and a fluid power pump. The simplifying assumptions for each model derivation are clearly stated at the beginning of each development.

Heat Exchangers

Most heat exchanger analyses are based on distributed-parameter, linear partial differential equations, the NTU (number of heat transfer units) method, or the log mean temperature difference (LMTD). Due to the complexities of distributed-parameter modeling, a simpler model is desired but not always obtained. While LMTD and NTU analyses are easier to perform than distributed-parameter analyses, more simplified analyses can be done by lumping the thermal capacitance and the thermal conductance of an exchanger into separate parameters and using the arithmetic mean temperature difference (AMTD) approximation to the LMTD of an exchanger. The criterion which must be met to ensure less than a ten per cent difference between the AMTD and the LMTD for a liquid-to-air or a liquid-to-liquid heat exchanger is given by Geidt (11) as follows:

$$\frac{T_{fi_H}}{T_{fi_H} - T_{amb_H}} > 9 \quad (1a)$$

or

$$\frac{T_{fi_L}}{T_{fi_L} - T_{co}} > 9 \quad (1b)$$

where all the temperatures must be in degrees Fahrenheit.

In the following pages, a liquid-to-air and a liquid-to-liquid heat

exchanger are modeled using the above approximations. The differences between the two models are that the thermal capacitance of the air (coolant) in the first case is assumed to be negligible in comparison to that of the liquid, and the exchanger has only one output. The capacitances of the coolant and the working fluid are considered in the second case while this exchanger has two outputs. The models are developed in a parallel fashion to show these differences.

The following assumptions are applicable for either or both types of heat exchangers:

- (1) Radiation effects are negligible.
- (2) The atmosphere serves as an infinite heat sink.
- (3) The thermal capacitance and the thermal conductance can be lumped into two respective parameters (the latter of which is flow rate dependent (28)).
- (4) All the thermal energy brought in by the fluids is carried away by the fluids (i.e., there is no other method of heat transfer).
- (5) The specific heats of the working liquid and the cooling liquid are constant.
- (6) Two phase flow does not occur.

The steady-state and dynamic models derived below are invalid for low liquid flow rates since some of the terms of the model equations are inversely proportional to flow rate. Thus, as the flow rates approach zero, some of the terms would approach infinity, and the models would be invalid.

Figure 1(a) represents a liquid-to-air heat exchanger enclosed

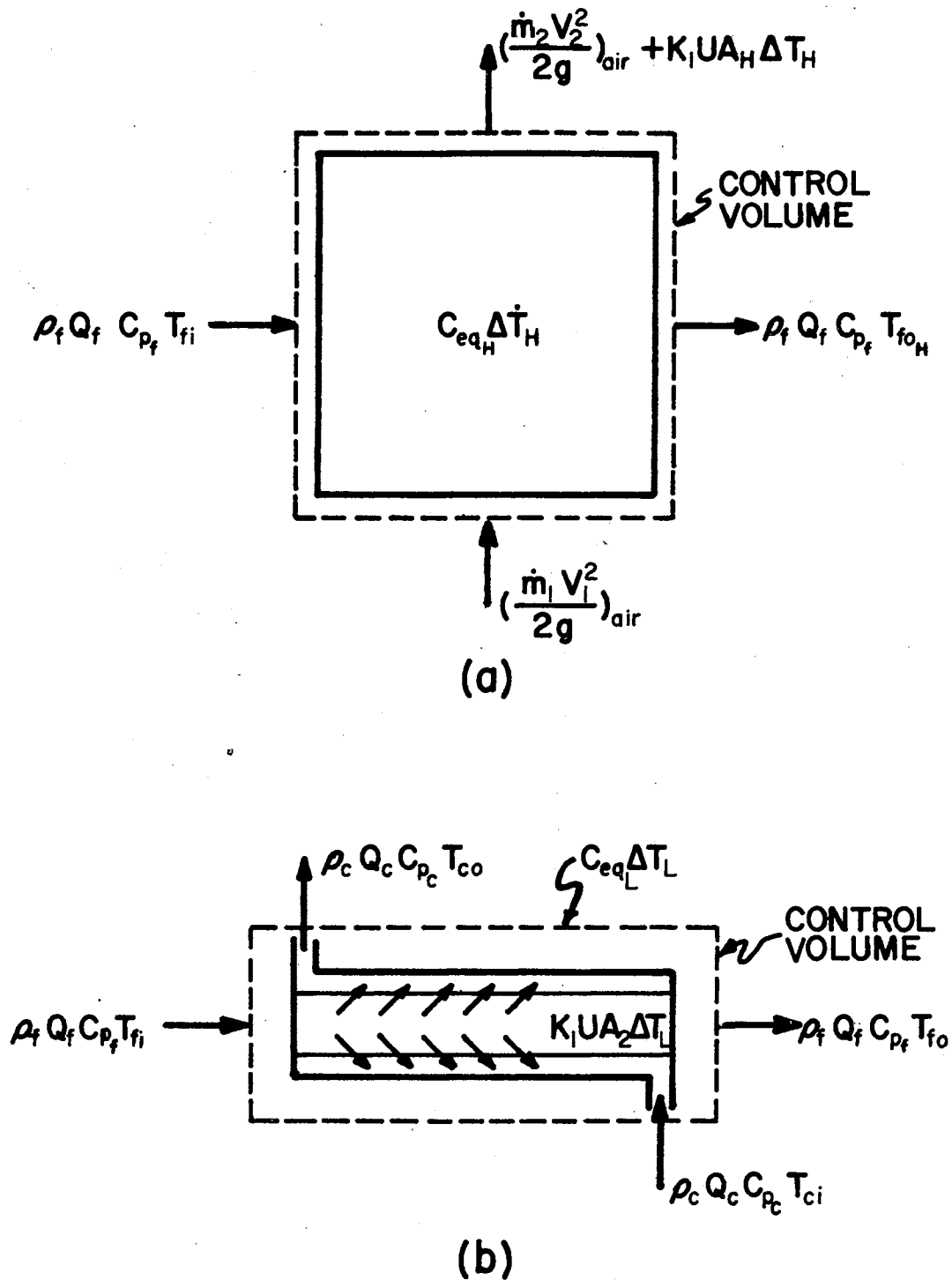


Figure 1. Representation of (a) a Liquid-to-Air Heat Exchanger, (b) a Liquid-to-Liquid Heat Exchanger.

within a control volume. The rates of energy entering, leaving, and being stored in the exchanger are shown in the figure (the notation used is defined in the list of nomenclature). The kinetic energy of the air moving through the heat exchanger is caused by a fan and is included to give a complete picture of the energy exchange. However, since the kinetic energy of the air is conserved, the following equation is obtained:

$$\frac{\dot{m}_1 V_1^2}{2g} \text{ air} = \frac{\dot{m}_2 V_2^2}{2g} \text{ air} \quad (2)$$

In order to minimize the number of parameters involved, it is assumed that the energy storage term of the liquid-to-liquid heat exchanger can be approximated by $Ceq_L \dot{T}_L$. This is approximately true if the bulk temperature of one fluid is constant. Hence, an energy balance for the exchanger is written as follows:

$$\rho_f Q_f C_p T_{fi_H} = Ceq_H \dot{\Delta T}_H + k_1 UA_H \Delta T_H + \rho_f Q_f C_p T_{fo_H} \quad (3)$$

where

$$\Delta T_H = \frac{T_{fi_H} + T_{fo_H}}{2} - T_{amb_H} \quad (4)$$

is defined as the AMTD of the exchanger.

Figure 1(b) represents a counter flow liquid-to-liquid heat exchanger and also shows the energy input, output, storage, and transfer rates of the exchanger. The products expressing these rates would be the same regardless of the exchanger configuration being considered.

An energy balance for the exchanger is written in two parts as follows:

$$\rho_f Q_f C_p T_{fi_L} = Ceq_L \dot{\Delta T}_L + k_1 UA_L \Delta T_L + \rho_f Q_f C_p T_{fo_L} \quad (5)$$

$$\rho_c Q_c C_{p_c} T_{ci} + k_1 UA_L \Delta T_L = \rho_c Q_c C_{p_c} T_{co} \quad (6)$$

where

$$\Delta T_L = \frac{T_{fi_L} + T_{fo_L}}{2} - \frac{T_{ci} + T_{co}}{2} \quad (7)$$

is defined as the AMTD of the heat exchanger.

To use state variable representation, each exchanger can be considered as a system having inputs, outputs, and a state vector (where the state of the system describes the outputs at any point in time). The quantities which are inputs to the exchangers are chosen to be Q_f , T_{fi_H} , T_{amb_H} , Q_c , T_{ci} , and T_{fi_L} . Having the inputs, the energy balances given by Equations (3), (5), and (6) can be used to derive steady-state and dynamic thermal models for the liquid-to-air and the liquid-to-liquid heat exchangers.

Steady-State Analysis

At steady-state conditions, the storage rate of thermal energy in the exchangers is zero, and the energy balances for the liquid-to-air and the liquid-to-liquid exchanger simplify to the following equations:

$$\rho_f Q_f C_{p_f} T_{fi_H} = k_1 UA_H \Delta T_H + \rho_f Q_f C_{p_f} T_{fo_H} \quad (8)$$

$$\rho_f Q_f C_{p_f} (T_{fi_L} - T_{fo_L}) = \rho_c Q_c C_{p_c} (T_{co} - T_{ci}) = k_1 UA_L \Delta T_L \quad (9)$$

From Equations (4) and (8), the steady-state outlet temperature of the liquid-to-air heat exchanger is obtained as follows:

$$T_{fo_H} = \frac{\left(1 - \frac{k_1 UA_H}{2\rho_f Q_f Cp_f}\right) T_{fi_H} + \frac{k_1 UA_H}{\rho_f Q_f Cp_f} T_{amb_H}}{1 + \frac{k_1 UA_H}{\rho_f Q_f Cp_f}} \quad (10)$$

The steady-state model for the liquid-to-liquid heat exchanger consists of two algebraic equations: one for the outlet temperature of the working liquid and one for the outlet coolant temperature. The first equality of Equation (9) gives the following:

$$T_{co} = T_{ci} + \frac{\rho_f Q_f Cp_f}{\rho_c Q_c Cp_c} (T_{fi_L} - T_{fo_L}) \quad (11)$$

Substituting this value for T_{co} and the value for ΔT_L from Equation (7) into the first and third parts of Equation (9) yields the steady-state outlet temperature of the working fluid:

$$T_{fo_L} = \frac{\frac{k_1 UA_L}{\rho_f Q_f Cp_f} T_{ci} + \left[1 - \frac{k_1 UA_L}{2\rho_f Q_f Cp_f} \left(1 - \frac{\rho_f Q_f Cp_f}{\rho_c Q_c Cp_c}\right)\right] T_{fi_L}}{1 + \frac{k_1 UA_L}{2\rho_f Q_f Cp_f} \left(1 + \frac{\rho_f Q_f Cp_f}{\rho_c Q_c Cp_c}\right)} \quad (12)$$

This quantity, when substituted into Equation (11), decouples the equations for T_{co} and T_{fo_L} , and the second equation of the steady-state model is obtained as follows:

$$T_{co} = T_{ci} + \frac{\rho_f Q_f Cp_f}{\rho_c Q_c Cp_c} \left[\frac{T_{fi_L} - \frac{k_1 UA_L}{\rho_f Q_f Cp_f} T_{ci} + \left[1 - \frac{k_1 UA_L}{2\rho_f Q_f Cp_f} \left(1 - \frac{\rho_f Q_f Cp_f}{\rho_c Q_c Cp_c}\right)\right] T_{fi_L}}{1 + \frac{k_1 UA_L}{2\rho_f Q_f Cp_f} \left(1 + \frac{\rho_f Q_f Cp_f}{\rho_c Q_c Cp_c}\right)} \right] \quad (13)$$

The steady-state thermal models for the liquid-to-air and the liquid-to-liquid heat exchangers are given by Equations (10), (12), and (13), respectively. The difference between the exchanger models is that the latter requires two equations since it has T_{co} and T_{foL} as outputs while the former has only one output, T_{foL} .

Dynamic Analysis

The basic equations for deriving dynamic thermal models for the two exchangers are given by Equations (3), (4), (5), (6), and (7). The only other definition needed for each exchanger is that of a state vector. ΔT_H and ΔT_L conveniently serve these purposes.

Considering the liquid-to-air heat exchanger first, a dynamic model can be derived from Equations (3) and (4). An algebraic expression for T_{foH} is obtained directly from the definition of the state vector ΔT_H , i.e.,

$$T_{foH} = 2(\Delta T_H + T_{amb_H}) - T_{fi_H} \quad (14)$$

Using this result in Equation (4) yields the following first-order non-linear differential equation:

$$\dot{\Delta T}_H = [2\rho_f Q C_{p_f} (T_{fi_H} - T_{amb_H}) - (2\rho_f Q C_{p_f} + k_1 U A_H) \Delta T_H] / C_{eq_H} \quad (15)$$

Simultaneous solution of Equations (14) and (15) gives the dynamic response of a liquid-to-air heat exchanger for any input or set of inputs.

A dynamic model for a liquid-to-liquid heat exchanger can be derived from Equations (5), (6), and (7). Rewriting Equation (6)

gives the outlet coolant temperature in terms of input quantities, component parameters, and the state vector ΔT_L :

$$T_{co} = T_{ci} + \frac{k_1 U A_L}{\rho_c Q_c C_{p_c}} \Delta T_L \quad (16)$$

By solving Equation (7) for T_{fo_L} and substituting for T_{co} given by Equation (16), gives T_{fo_L} also in terms of inputs, parameters, and the state vector ΔT_L , i.e.,

$$T_{fo_L} = 2 T_{ci} + \left(2 + \frac{k_1 U A_L}{\rho_c Q_c C_{p_c}} \right) \Delta T_L - T_{fi_L} \quad (17)$$

Substituting the quantity T_{fo_L} given by Equation (17) into Equation (5) results in the following first-order, nonlinear equation:

$$\dot{\Delta T}_L = \frac{2\rho_f Q_f C_{p_f}}{C_{eq_L}} (T_{fi_L} - T_{ci}) - \left[k_1 A_L + \rho_f Q_f C_{p_f} \left(2 + \frac{k_1 U A_L}{\rho_c Q_c C_{p_c}} \right) \right] \frac{\Delta T_L}{C_{eq_L}} \quad (18)$$

Equations (16), (17), and (18) constitute a lumped-parameter dynamic model for a liquid-to-liquid heat exchanger while a lumped-parameter model for a liquid-to-air exchanger is given by Equations (14) and (15). Simultaneous solution of these two sets of equations yields the predictions of the AMTD and the outlet temperatures of each exchanger at any point in time.

Reservoir

Perhaps the most influential component, excluding heat exchangers, on overall system thermal performance is the reservoir. In systems with no heat exchangers, the heat loss from a system is transferred from the

reservoir. Cases where this is not true are systems with long lines, with reservoirs that contain only a small volume of fluid, or with actuators that hold large volumes of fluid.

The simplifying assumptions for this analysis are tabulated below:

- (1) All heat loss occurs through the mechanism of convective heat transfer to the atmosphere (i.e., radiation effects are negligible).
- (2) The only addition of thermal energy to the reservoir is from incoming fluid (internal heating elements are not considered).
- (3) Perfect mixing of the fluid is assumed. This means that the bulk fluid temperature of the reservoir is approximated by the arithmetic mean of the inlet and outlet fluid temperatures.
- (4) All thermal conductance and capacitance effects can be lumped into two parameters, UA_R and C_{eqR} , respectively, and the former is flow rate dependent (28).

The above assumptions are general enough to enable the lumped-parameter modeling concept to be applicable to any reservoir. The case of internal reservoir heating can easily be handled by accounting for it in an energy balance.

Figure 2 represents any system reservoir in general, and an energy balance for the control volume includes four terms:

$$\rho_f Q_f C_{p_f} T_{fi_R} - \rho_f Q_f C_{p_f} T_{fo_R} = C_{eqR} \dot{\Delta T}_R + k_1 UA_R \Delta T_R \quad (19)$$

where:

$$\Delta T_R = \frac{T_{fi_R} + T_{fo_R}}{2} - T_{amb_R} \quad (20)$$

In Equations (19) and (20) inputs to the reservoir are defined as Q_f , T_{fi_R} , and T_{amb_R} for the same reasons given in the previous analyses. Using these definitions, steady-state and dynamic thermal models for any

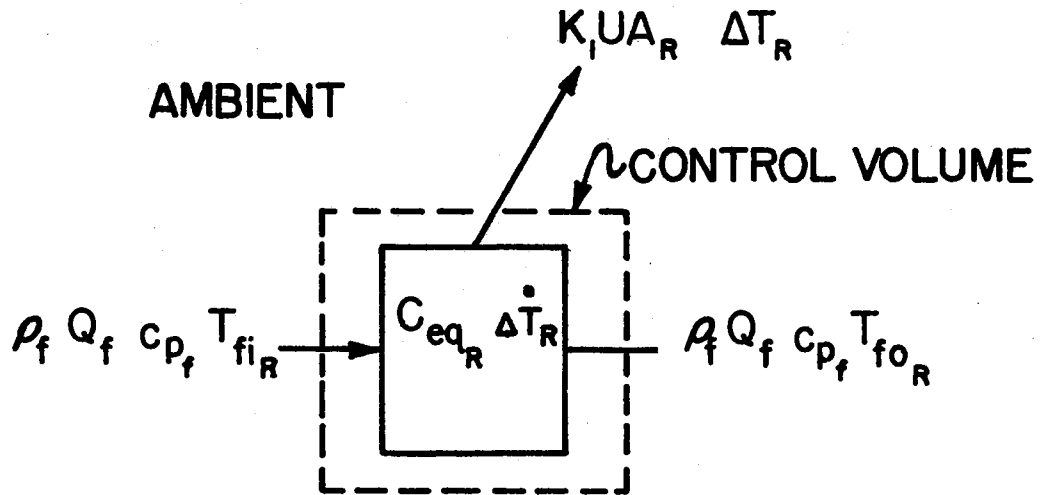


Figure 2. Representation of a Reservoir

reservoir can be derived.

Steady-State Analysis

At steady-state conditions, the capacitance term drops out of the energy balance and an expression for the outlet fluid temperature can be determined as a function of inputs and parameters, i.e.,

$$T_{foR} = \frac{\left(1 - \frac{UA_R}{2\rho_f Q_f C_{p_f}}\right) T_{fiR} + \frac{k_1 UA_R}{\rho_f Q_f C_{p_f}} T_{ambR}}{1 + \frac{UA_R}{\rho_f Q_f C_{p_f}}} \quad (21)$$

This equation represents the steady-state lumped-parameter thermal model for a reservoir.

Dynamic Analysis

To model the transient behavior of a reservoir, the heat storage capacity of the reservoir must be included in the analysis. Defining ΔT_R as the state vector of the reservoir for similar reasons to those of the analyses given earlier, an algebraic equation for the outlet fluid temperature can be written directly from Equation (20), i.e.,

$$T_{foR} = 2(\Delta T_R + T_{ambR}) - T_{fiR} \quad (22)$$

Substituting this quantity into the energy balance given by Equation (19) results in a first-order differential equation which describes the transient behavior of a reservoir:

$$\dot{\Delta T}_R = [2\rho_f C_{p_f}(T_{fiR} - T_{ambR}) - (k_1 UA_R + 2\rho_f C_{p_f})\Delta T_R]/C_{eqR} \quad (23)$$

Equations (22) and (23) form a dynamic thermal model which is applicable to any reservoir.

Fluid Power Pump

In performing any system analysis it is advantageous to have a qualitative knowledge of the steady-state and dynamic characteristics of the components which constitute the system. Based on this information, the components that are influential in the dynamics of a total system are often immediately apparent. This observation is for any system and is a necessary condition for lumped-parameter thermal analyses of fluid power systems. The significance of this generalization is shown below in a thermal analysis of a positive displacement pump.

The assumptions for the development of a lumped-parameter steady-state and dynamic thermal model for a pump are tabulated below. Most of the following assumptions were first presented by Ebbesen (6), who advanced the basic theory for a lumped-parameter, dynamic thermal model for a fluid power pump. The list of assumptions given here is more extensive than that given by Ebbesen, and the steady-state and dynamic models that are derived are considered to be refinements of this earlier work.

- (1) Radiation heat transfer is negligible.
- (2) The environment serves as an infinite heat sink.
- (3) The external pump wall temperature is the bulk temperature of the pump body.
- (4) The bulk temperature of the fluid in the pump is approximated by the arithmetic mean of the inlet and outlet fluid temperatures (i.e., perfect mixing is assumed).

- (5) The fluid is incompressible and frictionless.
- (6) Kinetic and potential energy due to elevation are negligible.
- (7) The bulk temperature of the fluid contained by the pump exceeds the pump body temperature. The basis for this assumption is that pump inefficiency is due principally to the viscous shearing of the hydraulic fluid. Consequently, thermal energy is generated by the fluid and then transferred to the pump body.
- (8) It is assumed that the case drain can be connected to the pump outlet. The pump outlet temperature is then the fluid temperature immediately downstream of the connection (i.e., perfect mixing occurs at the connection).

A thermal analysis of a fluid power pump can be divided into two separate parts: (1) an energy balance for the pump body, and (2) an energy balance for the fluid. In accordance with the above assumptions the energy balances are written as follows:

$$\text{Pump body: } k_1 UA_f \Delta T_f = Ceq_w \dot{\Delta T}_w + k_1 UA_w \Delta T_w \quad (24)$$

$$\begin{aligned} \text{Fluid: } Ceq_f \dot{\Delta T}_f + k_1 UA_f \Delta T_f &= k_2 Q_f \Delta P \left(\frac{1-\eta}{\eta} \right) \\ &+ \rho_f Q_f C_{p_f} (T_{fi_p} - T_{fo_p}) \end{aligned} \quad (25)$$

where:
$$\Delta T_w = T_w - T_{amb_p} \quad (26)$$

$$\Delta T_f = \frac{T_{fi_p} + T_{fo_p}}{2} - T_w \quad (27)$$

Equations (26) and (27) are approximations to the temperature differences since T_w and the mean of the inlet and outlet fluid temperatures are also approximations.

The inputs for the steady-state and dynamic models are defined from Equations (24) and (25) as Q_f , ΔP , T_{fi_p} , and T_{amb_p} , while the outputs are the pump wall temperature and the outlet fluid temperature. This information is sufficient for performing steady-state or dynamic thermal analyses of a fluid power pump.

Steady-State Analysis

At steady-state operating conditions, the energy balances for the pump body and the fluid, respectively, reduce to the following equations:

$$UA_f \Delta T_f = UA_w \Delta T_w \quad (28)$$

$$k_1 UA_f \Delta T_f = k_2 Q_f \Delta P \left(\frac{1-\eta}{\eta} \right) + \rho_f Q_f C_{p_f} (T_{fi_p} - T_{fo_p}) \quad (29)$$

Using the quantities defined by Equations (26) and (27) in (28) yields an equation for the pump body temperature in terms of the outlet fluid temperature. A similar substitution of ΔT_f into Equation (29) gives an algebraic expression for the outlet fluid temperature as a function of inputs and component parameters, i.e.,

$$T_{fo_p} = \frac{\rho_f Q_f C_{p_f} - \frac{k_1 UA_f UA_w}{2(UA_f + UA_w)} T_{fi_p} + \frac{k_1 UA_f UA_w}{(UA_f + UA_w)} T_{amb_p} + k_2 Q_f \Delta P \left(\frac{1-\eta}{\eta} \right)}{\rho_f Q_f C_{p_f} + \frac{k_1 UA_f UA_w}{2(UA_f + UA_w)}} \quad (30)$$

Substituting this result into the intermediate equation for the pump body temperature gives the second of the two equations which represent the steady-state thermal model for a pump:

$$T_w = \frac{UA_f}{2(UA_f + UA_w)} \left[\frac{\rho_f Q_f C_{p_f} - \frac{k_1 UA_f UA_w}{2(UA_f + UA_w)} T_{fi_p} + \frac{k_1 UA_f UA_w}{(UA_f + UA_w)} T_{amb_p} + k_2 Q_f \Delta P \left(\frac{1-\eta}{\eta} \right)}{\rho_f Q_f C_{p_f} + \frac{k_1 UA_f UA_w}{2(UA_f + UA_w)}} \right] + \frac{UA_w}{(UA_f + UA_w)} T_{amb_p} + \frac{UA_f}{2(UA_f + UA_w)} T_{fi_p} \quad (31)$$

Dynamic Analysis

Before any dynamic analysis can be done a state vector must be defined for the pump. $\begin{bmatrix} \Delta T_f \\ \Delta T_w \end{bmatrix}$ is defined as the state vector for the pump to minimize the manipulation of equations. Two algebraic equations which are part of the dynamic model are obtainable directly from Equations (26) and (27), i.e.,

$$T_w = \Delta T_w + T_{amb_p} \quad (32)$$

$$T_{fo_p} = 2(\Delta T_w + \Delta T_f + T_{amb_p}) - T_{fi_p} \quad (33)$$

The differential equations for the model are obtained from substituting T_w and T_{fo_p} into Equations (23) and (24). The results of these

substitutions are given by two first-order, coupled differential equations that are as follows:

$$\dot{\Delta T}_f = \frac{k_2 Q_f \Delta P (1 - \eta)}{\eta} + 2 \rho_f Q_f C_{p_f} (T_{fip} - \Delta T_w - T_{amb_p}) - (2 \rho_f Q_f C_{p_f} + k_1 UA_f) \Delta T_f / C_{eq_f} \quad (34)$$

$$\dot{\Delta T}_w = k_1 (UA_f \Delta T_f - UA_w \Delta T_w) / C_{eq_w} \quad (35)$$

Equations (32) through (35) form the dynamic thermal model for a fluid power pump.

The following chapter incorporates some of the component models derived in this chapter in the development of total system models.

CHAPTER IV

DEVELOPMENT OF STEADY-STATE AND DYNAMIC MODELS FOR COMPLETE SYSTEMS

There are two approaches to the formulation of lumped-parameter thermal models: (1) the system can be modeled as a whole or (2) a system model can be derived by combining component models. Examples of each are presented in the following pages.

Two open-center system configurations are presented, and steady-state and dynamic thermal models are derived for each. The systems that are treated are an open-center system without a heat exchanger and with a liquid-to-air heat exchanger. The components comprising the system are a positive displacement pump, a relief valve, a four way open-center directional control valve, and a load valve (needle valve) across the work ports of the directional control valve. A schematic of the system without heat exchangers is given in Figure 3.

The assumptions applicable to each development are stated prior to the derivations of the system models.

Total System Without Heat Exchangers

This system will be modeled using the first approach mentioned above. Thermal analysis of a total system differs slightly from individual component thermal analyses in that more terms enter into an

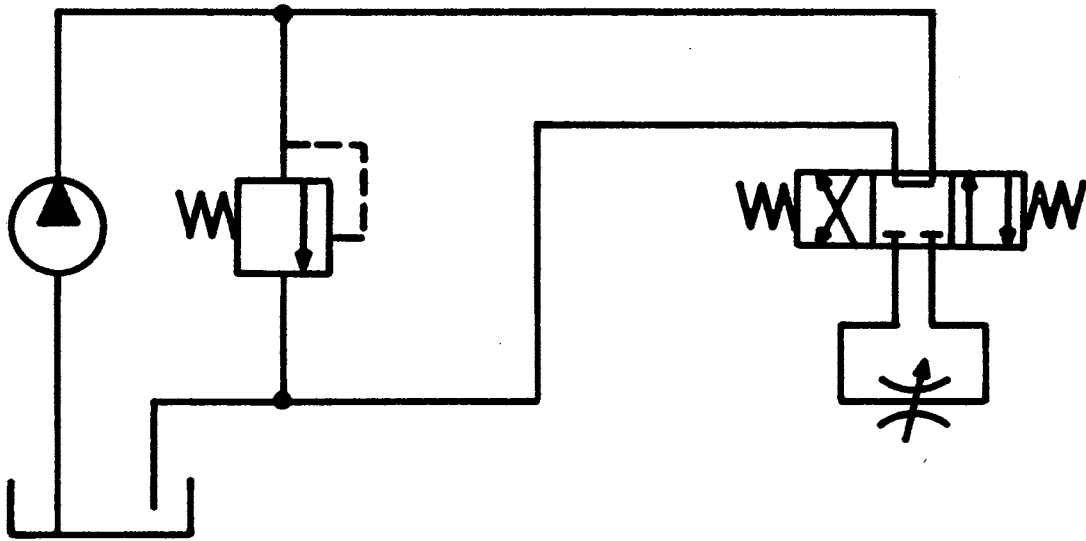


Figure 3. Schematic of an Open-Center System Without a Heat Exchanger

energy balance for a complete system than for a single component. Consequently, the steady-state and dynamic thermal models may become more complex than those for a component.

The simplifying assumptions for the formulation of thermal models for the system illustrated in Figure 3 are listed below:

- (1) All frictional losses due to component inefficiencies can be considered as heat addition to the system.
- (2) The working fluid is incompressible.
- (3) All heat is transferred to the surroundings from the reservoir; a constant overall heat transfer coefficient is applicable to the reservoir.
- (4) The thermal capacitance and thermal conductance of the system can be lumped into one component, the reservoir.
- (5) The pump acts only as a constant heat source in addition to pressurizing the fluid. All the input energy not used for this purpose is converted to heat.
- (6) There is no flow through the relief valve.
- (7) The bulk temperature of fluid in the reservoir is the arithmetic mean of the inlet and outlet fluid temperature.
- (8) The outlet fluid temperature of one component serves as the inlet fluid temperatures to the next (i.e., heat transfer from interconnecting lines is negligible).
- (9) The environment acts as an infinite heat sink.

An energy balance for the system is obtained by analogizing this thermal system to an electrical system and applying Kirchoff's current law to the circuit. In such an analysis three distinct quantities enter

into the energy balance for the system. The first is the heat added within the system by component inefficiencies; the second is the heat transferred from the system to the environment; and the last, thermal energy stored in the capacitance of the system.

To obtain a thermal model for the system, the heat addition transfer, and storage rates of the system must be defined. These definitions are provided by the following equation:

$$\Sigma H_g = Ceq_R \dot{\Delta T}_R + k_1 UA_R \Delta T_R \quad (36)$$

where ΔT_R is defined by (20). From Figure 3 it can be seen that the temperature of the fluid entering the reservoir at any point in time is the reservoir outlet temperature plus the temperature increase caused by the addition of thermal energy as the fluid passes through the system. This is represented by the following equation:

$$T_{fi_R} = T_{fo_R} + \frac{\Sigma H_g}{\rho_f Q_f C_{p_f}} \quad (37)$$

To ascertain the total rate of rate addition, ΣH_g , it is useful to consider the wheatstone bridge analogy of an open-center directional control valve. This analogy is depicted in Figure 4, and the sources of thermal energy in the system are recognizable. The amount of thermal energy added to the system is the sum of the heat added by the orifices and the pump. The thermal energy added per unit time by each element is given below:

$$\text{Pump:} \quad Q_f \left(\frac{1-\eta}{\eta} \right) (P_S - P_T) k_2$$

$$\text{Orifice 1:} \quad Q_1 (P_S - P_A) k_2$$

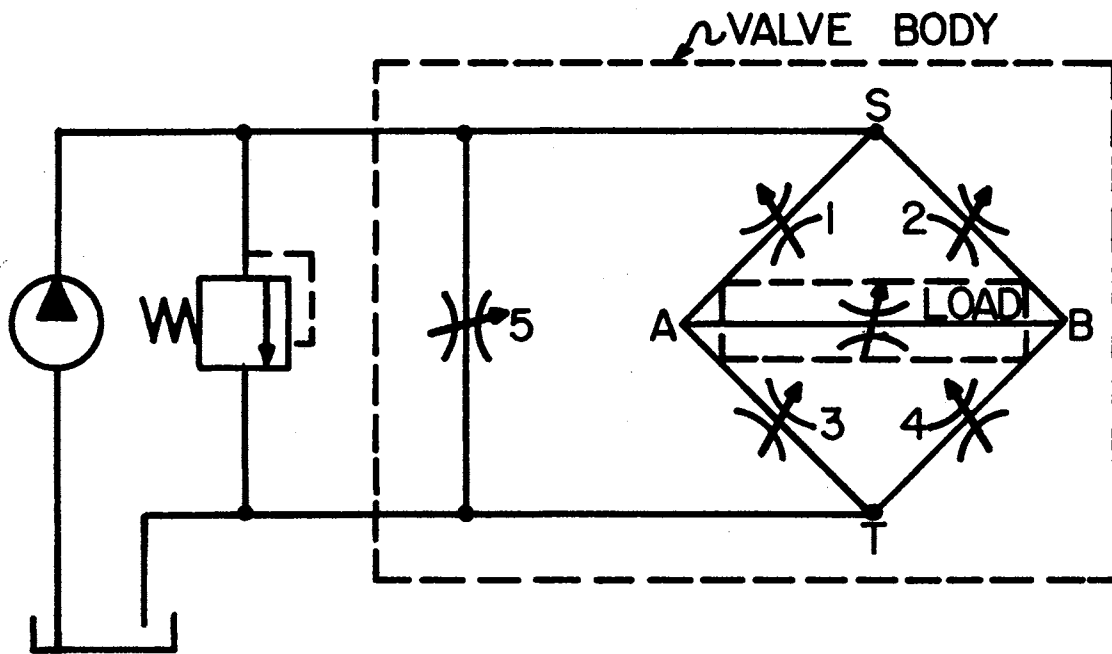


Figure 4. Wheatstone Bridge Analogy of an Open-Center Directional Control Valve

$$\text{Orifice 2: } Q_2(P_S - P_B)k_2$$

$$\text{Load: } Q_1 P_L k_2, x > 0$$

$$Q_2 P_L k_2, x < 0$$

$$P_L = \text{sgn}\{x\} |P_A - P_B|$$

$$x > 0, Q_1 = Q_4, Q_2 = Q_3 = 0$$

$$x < 0, Q_2 = Q_3, Q_1 = Q_4 = 0$$

$$\text{Orifice 3: } Q_2(P_A - P_T)k_2$$

$$\text{Orifice 4: } Q_1(P_B - P_T)k_2$$

$$\text{Orifice 5: } Q_5(P_S - P_T)k_2$$

From these definitions, the total rate of thermal energy added to the system is written as follows:

$$\begin{aligned} \Sigma Hg = k_2 [& Q_f \left(\frac{1-\eta}{\eta} \right) (P_S - P_T) + Q_1 \{ (P_S - P_A) + (P_B - P_T) \} + Q_2 \{ (P_S - P_B) \\ & + (P_A - P_T) \} + P_L (Q_1 + Q_2) + Q_5 (P_S - P_T)] \end{aligned} \quad (38)$$

The values for P_S , P_A , P_B , Q_1 , Q_2 , and Q_5 can be determined if supply flow rate Q_f , spool displacement x , and valve load, P_L , are known. A modified version of the open-center valve computer program developed by Iyengar and Miller (16) is capable of calculating the unknown flow rates and pressures as well as computing the rate of heat generated by the system.

The preceding discussion is also relevant for cyclic operation of the system (i.e., the inputs vary in a periodic fashion). The thermal energy added by one cycle can be calculated from Equation (38) by using the average flow rates and pressures for one cycle. Consequently, the

average rate of thermal energy added to the system is a constant for a given length of time for both constant and cyclic system loading.

System inputs are defined as supply flow rate Q_f , differential pump pressure $(P_S - P_T)$, valve spool displacement x , system load, P_L , and ambient temperature T_{amb_R} . Steady-state and dynamic thermal models for an open-center system without heat exchangers can now be derived.

Steady-State Analysis

In steady-state operation the energy balance for the system reduces to the following equality:

$$\rho_f Q_f C_{p_f} (T_{fi_R} - T_{fo_R}) = k_1 U A_R \Delta T_R \quad (39)$$

From this and Equation (20), the outlet fluid temperature of the reservoir is obtained as a function of system inputs and inlet reservoir temperature as follows:

$$T_{fo_R} = \frac{(2\rho_f Q_f C_{p_f} - k_1 U A_R) T_{fi_R} + 2k_1 U A_R T_{amb_R}}{(2\rho_f Q_f C_{p_f} + k_1 U A_R)}$$

Using Equation (37), the expression for the reservoir outlet fluid temperature is as follows:

$$T_{fo_R} = T_{amb_R} + \left(\frac{1}{k_1 U A_R} - \frac{1}{2\rho_f Q_f C_{p_f}} \right) \Sigma H_g \quad (40)$$

Combining Equations (37) and (40) yields an algebraic equation for the inlet temperature to the reservoir:

$$T_{fi_R} = T_{amb_R} + \left(\frac{1}{k_1 U A_R} + \frac{1}{2\rho_f Q_f C_{p_f}} \right) \Sigma H_g \quad (41)$$

Equations (40) and (41) form the steady-state thermal model for the system shown in Figure 4.

Dynamic Analysis

To perform a dynamic analysis, a state vector must be defined for the system. ΔT_R is a suitable quantity to consider as a state vector since using this quantity as the state vector minimizes the algebra in formulating a dynamic model. An expression for the outlet reservoir temperature is obtained by substituting T_{fi_R} given by Equation (37) into Equation (20). Solving for T_{fo_R} yields the following result:

$$T_{fo_R} = \Delta T_R + T_{amb_R} - \frac{\Sigma H_g}{2\rho_f Q_f C_{p_f}} \quad (42)$$

Using this expression for T_{fo_R} , an equation for the inlet reservoir is obtained from Equation (37) as the following:

$$T_{fi_R} = \Delta T_R + T_{amb_R} + \frac{\Sigma H_g}{2\rho_f Q_f C_{p_f}} \quad (43)$$

The differential equation for the system results from rewriting Equation (36) as follows:

$$\dot{\Delta T}_R = (\Sigma H_g - k_1 U A_R \Delta T_R) / C_{eq_R} \quad (44)$$

It should be noted that the average rate of thermal energy added to the system is constant if the supply flow rate is constant. Then the differential equation given by (44) is a linear, ordinary differential equation that has an exact solution. This solution is written below:

$$\Delta T_R(t) = \frac{\Sigma Hg}{k_1 U A_R} + \left(\Delta T_R(0) - \frac{\Sigma Hg}{k_1 U A_R} \right) e^{-\frac{k_1 U A_R}{Ceq_R} t} \quad (45)$$

where $\Delta T_R(0)$ is a known initial condition.

Total System With a Liquid-to-Air

Heat Exchanger

The model development here will follow the second scheme indicated at the beginning of the chapter. Addition of a liquid-to-air heat exchanger to the open-center system of Figure 4 results in a more general and a more complex system. The lumped-parameter modeling techniques used previously are still applicable and are considerably less cumbersome than a distributed-parameter model would be. Figure 5 shows a schematic of an open-center system with a liquid-to-air heat exchanger.

The assumptions for analyzing the system given in Figure 4 have been stated for the cases of the liquid-to-air heat exchanger and the preceding total system analysis.

To perform a lumped-parameter analysis of the system, it is advantageous to model the system in two parts: (1) the heat exchanger, and (2) the remaining components of the system. The energy balances that are obtained by dividing the system in this manner are given by Equations (3), (44), and the following equation:

$$\rho_f Q_f C_{p_f} T_{fi} = \rho_f Q_f C_{p_f} T_{fo_R} + \Sigma Hg \quad (46)$$

In Equation (20), the inlet reservoir temperature T_{fi_R} is T_{fo_H} system. The only changes that occur because of the combination of these

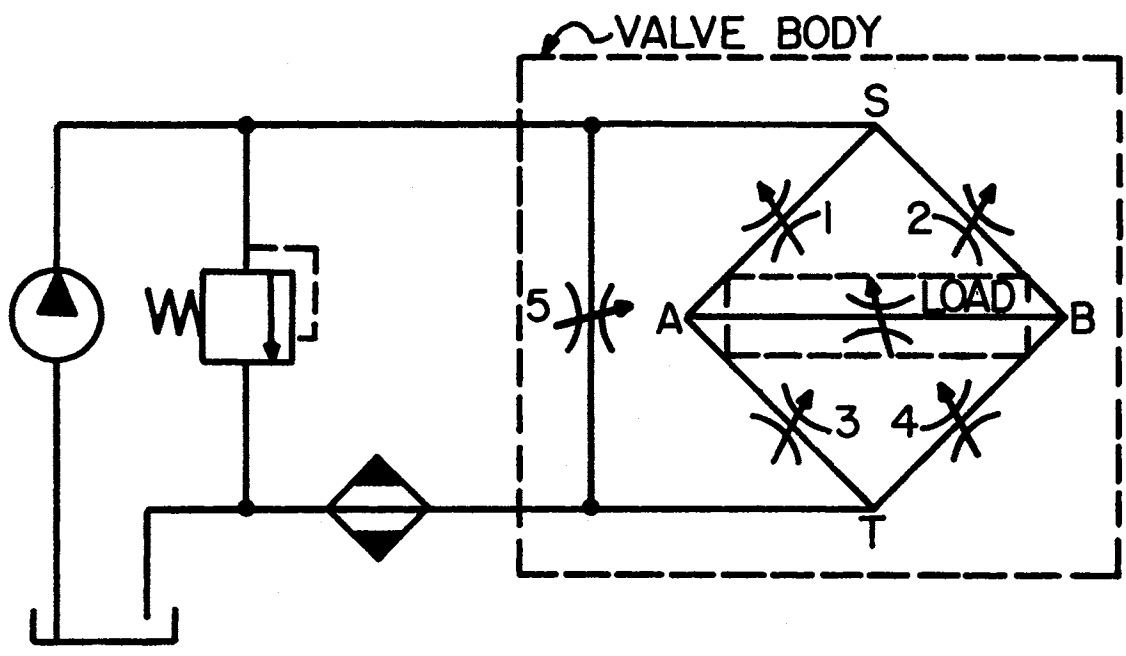


Figure 5. Open-Center System With a Liquid-to-Air Heat Exchanger

two models are the system inputs. The inputs to the system are Q_f , ΔP , x , P_L , ΣH_g , T_{amb_H} , and T_{amb_R} . With the inputs and energy balance equations defined, steady-state and dynamic thermal analyses can be done.

Steady-State Analysis

At steady-state conditions, the storage rates of thermal energy are zero, and the energy balance for the system simplifies to the following equations:

$$\rho_f Q_f C_{p_f} (T_{fi_H} - T_{fo_H}) = k_1 UA_H \Delta T_H \quad (47)$$

$$\rho_f Q_f C_{p_f} (T_{fo_H} - T_{fo_R}) = k_1 UA_R \Delta T_R \quad (48)$$

Substitution of ΔT_H and ΔT_R into Equations (47) and (48) result in algebraic equations for the steady-state temperatures at the inlet and outlet ports of the exchanger and the reservoir.

Exchanger inlet:

$$T_{fi_H} = \frac{1}{2\rho_f Q_f C_{p_f} (UA_H + UA_R) k_1} \left[k_1 UA_R (2\rho_f Q_f C_{p_f} - k_1 UA_R) T_{amb_H} + k_1 UA_H (2\rho_f Q_f C_{p_f} + k_1 UA_R) T_{amb_R} + \frac{\Sigma H_g (2\rho_f Q_f C_{p_f} + k_1 UA_R) (2\rho_f Q_f C_{p_f} + k_1 UA_H)}{2\rho_f Q_f C_{p_f}} \right] \quad (49)$$

Exchanger outlet (reservoir inlet):

$$T_{fo_H} = \frac{2k_1 UA_H}{(2\rho_f Q_f C_{p_f} + k_1 UA_H)} T_{amb_H} + \frac{(2\rho_f Q_f C_{p_f} - k_1 UA_H)}{2\rho_f Q_f C_{p_f} k_1 (UA_H + UA_R) (2\rho_f Q_f C_{p_f} + k_1 UA_H)} \left[k_1 UA_H (2\rho_f Q_f C_{p_f} - k_1 UA_R) T_{amb_H} + k_1 UA_R (2\rho_f Q_f C_{p_f} + k_1 UA_R) T_{amb_R} + \frac{\Sigma H_g (2\rho_f Q_f C_{p_f} + k_1 UA_R) (2\rho_f Q_f C_{p_f} + k_1 UA_H)}{2\rho_f Q_f C_{p_f}} \right] \quad (50)$$

Reservoir outlet:

$$\begin{aligned}
 T_{fo_R} = & \frac{1}{2\rho_f Q_f C_{p_f} k_1 (UA_H + UA_R)} \left[k_1 UA_H (2\rho_f Q_f C_{p_f} - k_1 UA_R) T_{amb_H} \right. \\
 & + k_1 UA_R (2\rho_f Q_f C_{p_f} + k_1 UA_H) T_{amb_R} \\
 & \left. + \Sigma Hg \left[\frac{(2\rho_f Q_f C_{p_f} + k_1 UA_R)(2\rho_f Q_f C_{p_f} + k_1 UA_H) - 4\rho_f Q_f C_{p_f} k_1 (UA_H + UA_R)}{2\rho_f Q_f C_{p_f}} \right] \right]
 \end{aligned}
 \tag{51}$$

Equations (49), (50), and (51) comprise the steady-state model for an open-center system with a liquid-to-air heat exchanger.

Dynamic Analysis

The previous dynamic models that have been presented have state vectors defined in terms of differential temperatures in order to minimize the complexity of the models. The dynamic model for the system considered here deviates from this procedure by using absolute temperature. If the differential temperature approach was employed, the algebraic equations that are part of the dynamic model cannot be easily decoupled.

The system formed by combining the heat exchanger and the open-center system contains two thermal capacitances, but in spite of this the system is not second-order. This is demonstrated in Appendix A. The inlet temperature to the exchanger is defined as the state vector for the system and enables the decoupling of the algebraic equations for the model. A first-order differential equation model results from using the heat exchanger inlet temperature as the state vector.

The rate of thermal energy added to the system is a constant for

constant or cyclic loading conditions if the system flow rate is constant. In the following development it is assumed that these two inputs are constant.

Substituting ΔT_H and ΔT_R into Equations (3) and (44) gives two differential equations for the inlet exchanger temperature in terms of exchanger and reservoir outlet temperatures. The reservoir outlet temperature is eliminated by solving Equation (46) for it and substituting this result into both differential equations. Equating the differential equations gives the outlet exchanger temperature as a function of the state variable T_{fi_H} , system inputs, and system parameters:

$$T_{fo_H} = \frac{Ceq_H(2\rho_f Q_f Cp_f + k_1 UA_R) + Ceq_R(2\rho_f Q_f Cp_f - k_1 UA_H)}{Ceq_H(2\rho_f Q_f Cp_f - k_1 UA_R) + Ceq_R(2\rho_f Q_f Cp_f + k_1 UA_H)} T_{fi_H} - \left[\frac{\Sigma Hg \left(2 + \frac{k_1 UA_R}{\rho_f Q_f Cp_f} \right) Ceq_H + 2k_1 (UA_R Ceq_H T_{ambR} - UA_H Ceq_R T_{ambH})}{Ceq_H(2\rho_f Q_f Cp_f - k_1 UA_R) + Ceq_R(2\rho_f Q_f Cp_f + k_1 UA_H)} \right] \quad (52)$$

An algebraic equation for the reservoir outlet temperature is obtained by rewriting Equation (46) as follows:

$$T_{fo_R} = T_{fi_H} - \frac{\Sigma Hg}{\rho_f Q_f Cp_f} \quad (53)$$

Differentiating Equation (52) and substituting for \dot{T}_{fo_H} into one of the previously mentioned differential equations gives the following first-order differential equation for the exchanger inlet temperature:

$$\dot{T}_{fi_H} = - \frac{k_1 (UA_H + UA_R)}{(Ceq_H + Ceq_R)} T_{fi_H} + \left[\frac{Ceq_R (2\rho_f Q_f Cp_f + k_1 UA_H) \left\{ 2k_1 UA_R T_{amb_R} + \Sigma Hg \left(2 + \frac{k_1 UA_R}{\rho_f Q_f Cp_f} \right) \right\}}{4\rho_f Q_f Cp_f} \right. \\ \left. + \frac{k_1 (2\rho_f Q_f Cp_f - k_1 UA_R) (Ceq_H UA_R T_{amb_H} + Ceq_R UA_H T_{amb_R})}{(Ceq_H + Ceq_R) Ceq_R} \right] \quad (54)$$

To solve this set of equations, the inputs, system parameters, and initial condition for the exchanger inlet temperature must be known.

The scope of the experimental testing program presented in the following chapter is to provide steady-state and dynamic test data for identifying parameters for component and system models. Another major goal is to verify the dynamic models that have been presented in Chapters III and IV. Included in the verification of the models is the substantiation of the general lumped-parameter dynamic thermal modeling technique. It is also desired to verify that systems can be modeled by interfacing component models or by modeling the system as a whole.

CHAPTER V

EXPERIMENTAL VERIFICATION

There are several basic goals of experimental thermal testing. Steady-state data are invaluable for some parameter identification and often serve as the basis for dynamic model formulation. Dynamic test data are used for identifying component and system dynamic models and test the accuracy of the models. If experimental data and analytical predictions differ, there are two reasons for the discrepancies: (1) the model formulation is not accurate or (2) the parameter identification scheme was not successful. The modeling procedure can be repeated after appropriate corrective measures have been taken.

This chapter has two major subsections which include discussions of component steady-state and dynamic testing as well as total system testing. The identification of unknown component and system parameters from steady-state test data is also presented. Experimental data from dynamic thermal tests of various components and systems are compared to the predictions of their respective mathematical models. Close agreement between the measured data and predicted results verifies the mathematical model, while large discrepancies between the two indicate that the model is invalid, unsuitable for modeling the phenomenon, or incorrectly formulated. A discussion of the instrumentation used for the experimental testing program is given in Appendix B.

Component Testing

Liquid-to-Air Heat Exchanger

Liquid-to-air heat exchangers transfer thermal energy to the atmosphere by free convection or forced convection. Steady-state tests were conducted for both methods of heat transfer, and dynamic thermal tests were made for forced convection heat transfer only. Results of these tests are presented in the following section and are used to identify unknown parameters, which are later used to verify the lumped-parameter model that was derived in Chapter III.

Steady-State Tests

Several steady-state tests were run for different fluid flow rates through the test exchanger for free convection heat transfer. The inlet and outlet fluid and the ambient temperatures were recorded for every test. In all cases the outlet fluid temperature exceeded the inlet fluid temperature (i.e., the exchanger acted as a heat source).

Tests were run for the same flow rates with forced convection instead of free convection heat transfer. A circular fan with a constant angular velocity was the source of air flow over the heat exchanger. The fan was placed at such a distance that the entire frontal area of the exchanger was subjected to the air stream. The free stream velocity of the air was determined by taking the average of several velocity measurements at the heat exchanger surface. These measurements were made with a rotary anemometer.

Steady-state tests with forced convection heat transfer differed significantly from the natural convection tests. The outlet fluid

temperature was found always to be lower than the inlet temperature except for fluid flow rates greater than twenty gallons per minute. A number of tests were run using different fluid flow rates. The results of these tests were used to identify the thermal conductance of the component. Table I summarizes the steady-state test results and shows the UA_H for each test.

TABLE I
SUMMARY OF STEADY-STATE TESTS FOR A LIQUID-TO-AIR
HEAT EXCHANGER

Test #	Q_f	m_{air}	T_{fi_H}	T_{fo_H}	T_{amb_H}	UA_H
	gpm	cfm	$^{\circ}F$	$^{\circ}F$	$^{\circ}F$	Btu/hr/ $^{\circ}F$
1	3.87	2195	104.9	102.4	81.0	91.2
2	7.87	2195	97.7	97.3	81.5	38.4
3	7.93	2195	128.8	127.3	95.5	73.2
4	11.62	2195	115.7	114.5	78.8	83.4
5	15.32	2195	124.7	124.2	84.2	42.6
Average	---	--	---	---	--	65.8

It was noted in Reference (28) that the overall heat transfer coefficient U is flow rate dependent. Therefore the UA product also varies with flow rate. Since the range of flow rates used in all of the experimental testing was small (5 - 25 gpm), variations in UA were also

expected to be small. This justified the use of the average UA in the verification of the dynamic model for the liquid-to-air heat exchanger as well as the other dynamic models discussed in the following pages.

Dynamic Tests

Forced convection dynamic thermal tests were run with the input being an increase in the inlet fluid temperature generated by throttling the flow through a needle valve upstream of the exchanger. The fluid flow rate through and the flow rate of air across the heat exchanger were held constant. Different fluid flow rates were used for the various tests. The test run chosen for identifying C_{eq_H} was representative of all other tests (i.e., average flow rate, initial conditions, and air flow rate). An initial estimate of the thermal capacitance of the exchanger was made by taking the product of the specific heat and mass of the fluid contained in the component. This estimated value of C_{eq_H} and the average value of the conductance parameter from the steady-state tests were used in the simulation of Equations (14) and (15) to compare experimental and predicted temperatures. DYSIMP (8) was used for simulating the model. The simulation with the first estimate of C_{eq_H} gave good final values but large discrepancies in transients. Therefore, the specific heat times the mass of fluid in the heat exchanger was not a good estimate of the equivalent thermal capacitance of the exchanger.

Another approach to the identification of the capacitance parameter was taken by devising a simple Eulerian integration scheme to solve Equations (14) and (15). Since only one parameter needed to be identified, several hand calculations using this scheme converged upon a value of

19.82 Btu/°F for one test trajectory. This value was then used to simulate Equations (14) and (15) for all of the test conditions. The results of the simulations showed good agreement between computed values and experimental data. Table II gives a summary of the average, maximum, and final value errors between predicted and measured ΔT_H and T_{fo_H} . The data from test number 4 were used for identifying the thermal capacitance parameter. Figure 6 shows typical test results compared to analytical model predictions. The close agreement of the predicted and measured values shown in Figure 6 and summarized in Table II substantiate the lumped-parameter dynamic model for the test exchanger. The maximum transient error was 14.25 per cent while the maximum steady-state error was 3.66 per cent.

Since the dynamic model for the exchanger is first-order (equivalent to an RC electrical circuit), the time constant is determined by dividing the capacitance by the conductance (i.e., $\tau = 18.1$ minutes). The model is linear only if the fluid flow rate and the ambient temperature are constant.

Liquid-to-Liquid Heat Exchanger

A number of exchanger configurations have been designed to maximize exchanger effectiveness, which Parker et al. (25) define as the actual heat addition divided by the theoretical maximum heat addition for the cold fluid. Parallel flow, counter flow (which is the most effective design), and cross flow schemes as well as a combination of parallel and counter flow into multipass elements represent a few of many heat exchanger designs. The test exchanger was a 1 shell-2 tube pass, parallel-counter flow component with manufacturer's specifications of 132.8 square feet

TABLE II

ERROR SUMMARY FOR LIQUID-TO-AIR HEAT EXCHANGER SIMULATIONS

Test #	AMTD			Outlet Temperature		
	Average % Error	Maximum % Error	Final % Error	Average % Error	Maximum % Error	Final % Error
1	1.81	3.09	2.55	0.83	1.45	1.23
2	3.91	14.25	3.66	1.54	4.14	1.98
3	2.67	5.62	2.64	1.48	3.04	1.63
4	2.14	10.01	0.04	0.73	3.03	0.02
5	2.03	14.24	2.07	0.97	3.47	1.47
6	1.29	4.13	1.81	0.74	2.02	1.16

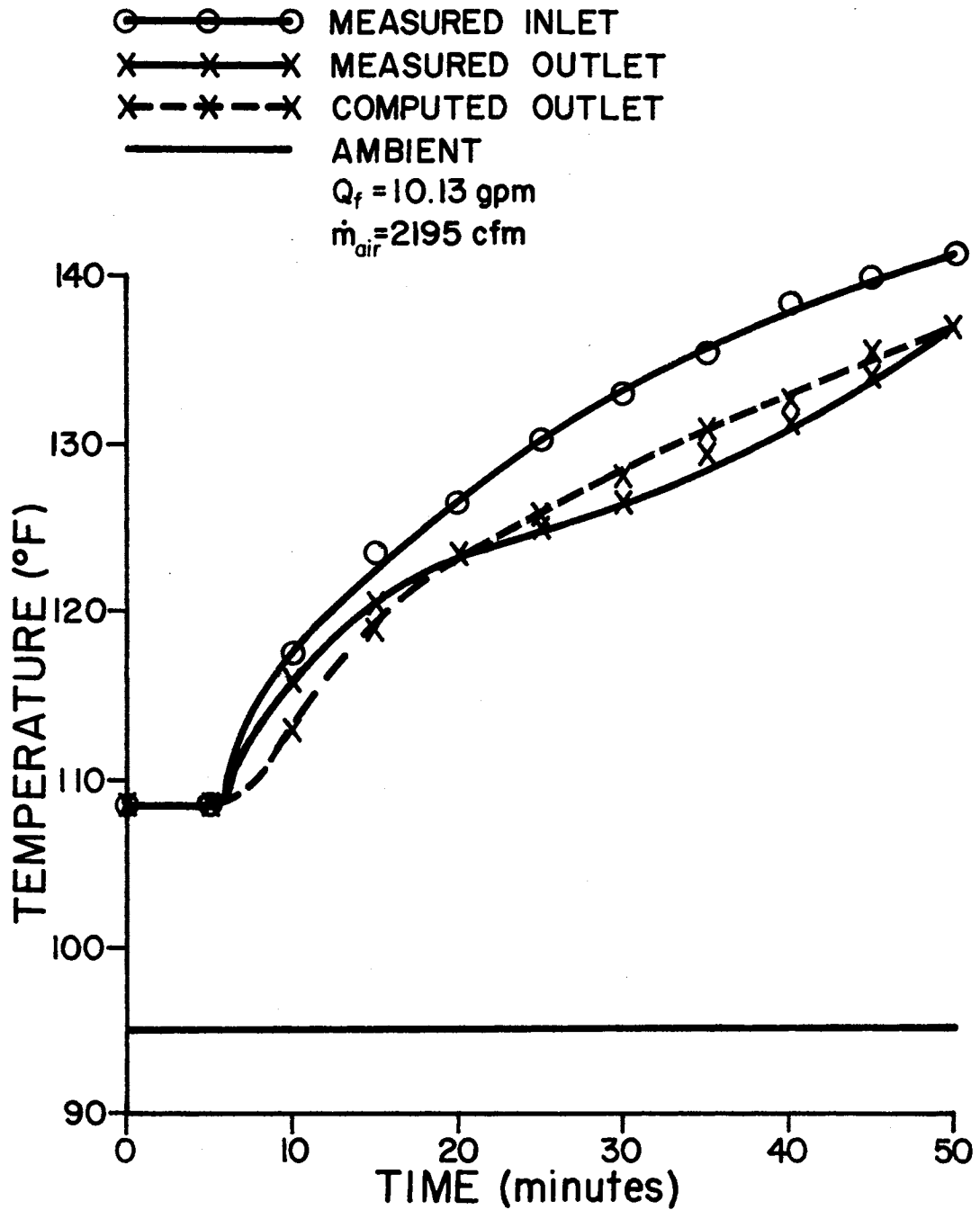


Figure 6. Liquid-to-Air Heat Exchanger Response to Increasing Inlet Fluid Temperature

for heat transfer, and an overall heat transfer coefficient of 100 Btu/hr/ft²/°F for all applications.

The exchanger was subjected to steady-state tests to determine the experimental lumped thermal conductance of the component. Dynamic tests were also run for the exchanger to identify the equivalent lumped thermal capacitance parameter.

Steady-State Tests

A series of steady-state test runs were made for various fluid and coolant flow rates through the exchanger. In all of the tests the hydraulic fluid flowed through the tube bundle and was throttled through a needle valve, while the coolant flowed through the shell side of the exchanger. The coolant and fluid flow rates and the inlet coolant temperature were constant for each test. Data recording was not begun until the inlet and outlet fluid and coolant temperatures stabilized at relatively constant values.

Coolant flow rates altered from zero to twenty gallons per minute while fluid flow rates ranged from five to forty gallons per minute. Four tests were run, and Equation (9) was used to calculate the thermal conductance for each test. Table III gives the calculated UA_L for each test as well as the average UA_L .

Comparison of the average UA_L of Table III with the manufacturer's specified UA_L of 1380 Btu/hr/°F shows a large disagreement between the two. Error in temperature measurements is the probable cause of the disagreement between the experimental and the specified UA_L . The experimental UA_L was used in verifying the dynamic model for the exchanger.

TABLE III
SUMMARY OF STEADY-STATE TESTS FOR A LIQUID-TO-LIQUID
HEAT EXCHANGER

Test #	Q_f	Q_c	T_{ci}	T_{co}	T_{fi}	T_{fo}	UA_L
	gpm	gpm	$^{\circ}F$	$^{\circ}F$	$^{\circ}F$	$^{\circ}F$	Btu/hr/ $^{\circ}F$
1	11.10	10.17	88.0	95.0	111.2	104.4	2212.8
2	13.21	9.18	88.0	104.0	134.6	122.0	2274.6
3	24.31	7.74	93.0	111.2	136.4	125.6	1219.2
4	24.44	10.29	90.0	105.8	136.4	123.8	2551.2
Average	--	--	--	--	--	--	2064.0

Dynamic Tests

The fluid and coolant flow rates were held constant for all of the tests, and a number of tests were run with increasing and decreasing fluid temperatures.

Dynamic test data can be used for identifying unknown parameters and in verifying the accuracy of the models. Using the value of UA_L determined from steady-state tests, the equivalent thermal capacitance parameter was identified in a manner similar to that of the liquid-to-air heat exchanger. One set of dynamic test data was used in a computer simulation for optimizing C_{eqL} . The parameter optimizing feature of DYSIMP (10) was used to determine C_{eqL} based on an integral squared error performance index of the following form:

$$PI = \int_{t_o}^{t_f} (\Delta T_{L_{meas}} - \Delta T_{L_{model}})^2 dt \quad (55)$$

The thermal capacitance parameter Ceq_L was found to be 17.916 Btu/°F and the value of the performance index was 18.477. From this value of Ceq_L and the experimental UA_L , the time constant for the exchanger was found to be 0.521 minutes with constant coolant and fluid flow rates and constant inlet coolant temperature constraints.

A computer simulation was done for each test using the above values of conductance and capacitance. The measured input data to the exchanger was used as an input to the model for simulation. An integration step size of 0.05 minutes was used in all of the computer simulations. An error analysis section was incorporated into the program to compare measured data with predicted values. The log mean temperature difference (LMTD) was calculated from raw data and compared to the AMTD that was predicted by the model. Table IV gives a summary of the average, maximum, and final value errors between predicted and measured outlet fluid and outlet coolant temperatures as well as a comparison of the LMTD with the AMTD. Test number 8 was the data set corresponding to the trajectory that was used to identify the thermal capacitance parameter.

Figures 7 and 8 show some typical results of the trajectories of the experimental and predicted temperatures for two different temperature inputs. Figure 9 shows the effect of a sudden increase in coolant flow rate through the heat exchanger. Although the effect this change had on the outlet coolant temperature was significant, it can be seen that the outlet fluid temperature was only slightly affected. The good agreement of the predicted and experimental results shown in these three

TABLE IV

ERROR BETWEEN EXPERIMENTAL DATA AND PREDICTED RESULTS FOR A
LIQUID-TO-LIQUID HEAT EXCHANGER

Run No.	Differences Between AMTD and LMTD			Outlet Coolant Temperature			Outlet Fluid Temperature		
	Average % Error	Maximum % Error	Final Value % Error	Average % Error	Maximum % Error	Final Value % Error	Average % Error	Maximum % Error	Final Value % Error
1		0.41	0.12	0.74	1.70	0.06	4.49	5.56	5.56
2	0.71	0.87	0.75	0.74	2.28	0.06	4.94	7.91	3.88
3	1.26	0.52	1.20	2.61	4.85	3.23	0.80	1.61	0.63
4	1.48	1.67	1.67	2.86	4.34	3.44	1.02	2.32	0.69
5	0.63	0.72	0.55	0.97	2.33	2.15	0.53	1.12	1.12
6	0.12	0.16	0.12	0.67	2.64	0.10	0.59	2.22	0.62
7	0.13	0.18	0.13	1.02	2.12	1.46	0.87	2.21	1.38
8	0.01	0.07	0.01	0.84	3.03	0.54	0.33	1.53	0.07
9	0.01	0.03	0.00	1.21	2.05	2.05	0.81	2.26	1.45
10	0.15	1.11	0.00	0.75	3.27	0.74	0.57	1.61	0.55

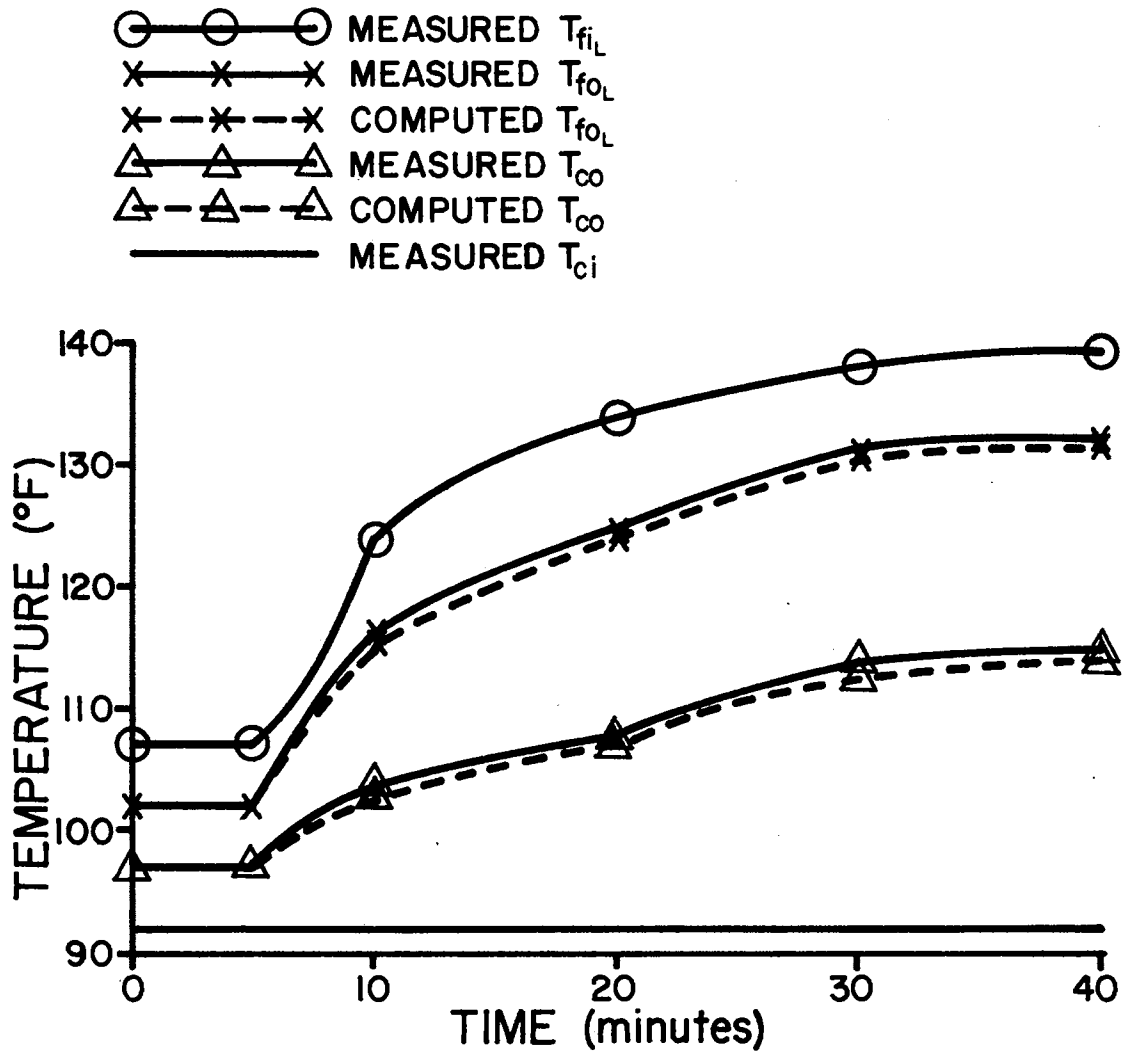


Figure 7. Typical Results for an Increase of Inlet Fluid Temperature

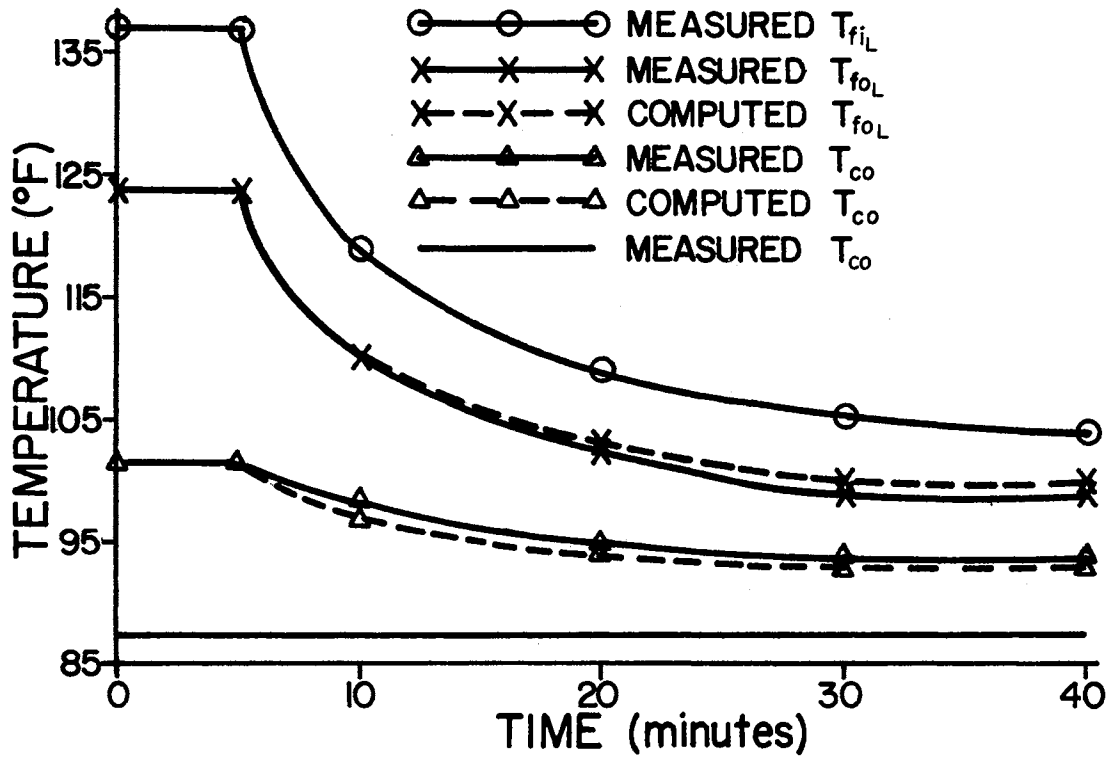


Figure 8. Typical Results for a Decrease of Inlet Fluid Temperature

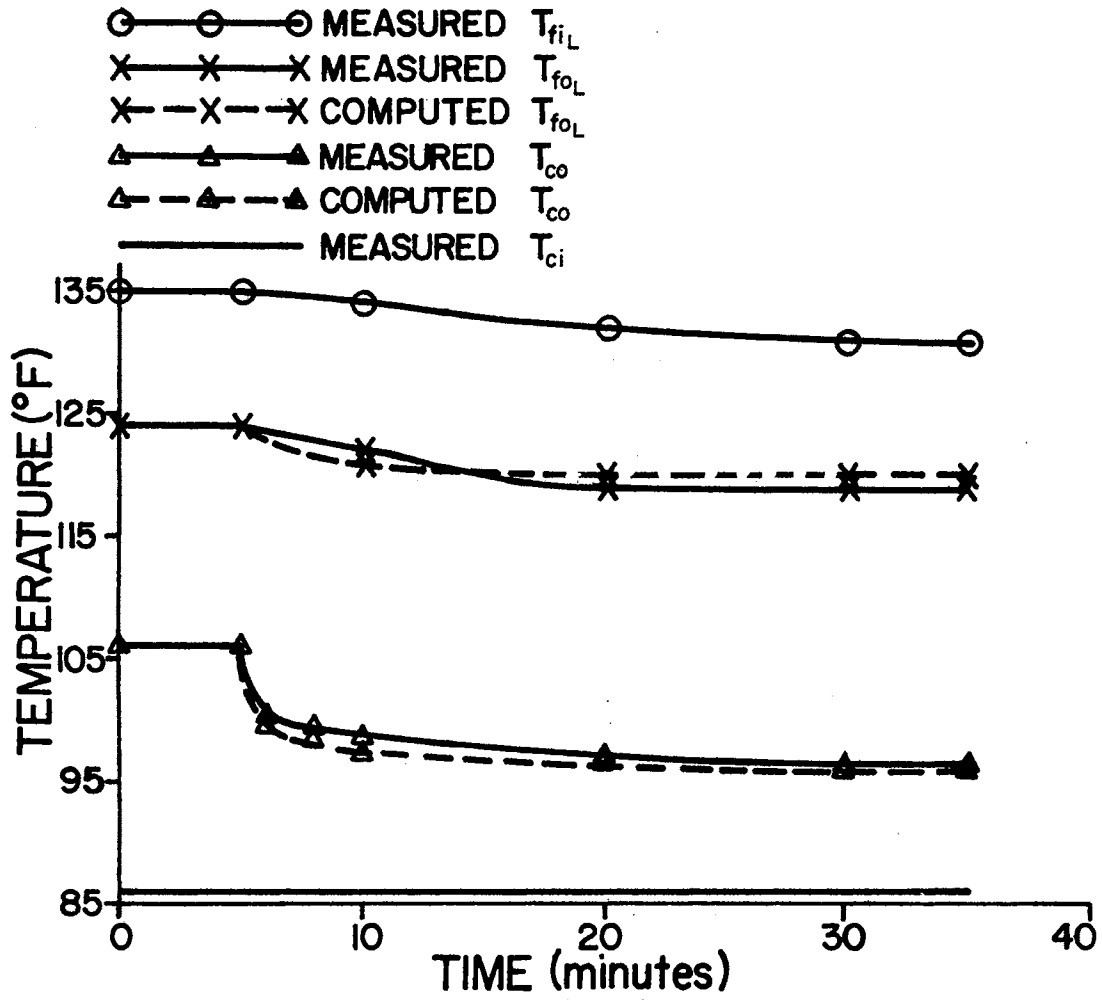


Figure 9. Effects of a Dynamic Change in Coolant Flow Rate Through the Heat Exchanger

figures and summarized in Table IV verifies the lumped-parameter dynamic model of a liquid-to-liquid heat exchanger.

The mathematical analysis of this type of heat exchanger is not as difficult as a distributed-parameter analysis, but it does provide a reasonably accurate dynamic model. The application of this simplified approach to thermal analysis of heat exchangers is useful to designers of fluid power systems.

Reservoir

Only steady-state tests were made for a hydraulic system reservoir, and these results are discussed below.

Three steady-state tests with different flow rates were conducted for the test reservoir. The results of these tests indicated little or no measurable difference between inlet and outlet fluid temperatures. No attempt was made to identify the lumped thermal conductance of the reservoir from the steady-state data since the differential temperatures between the inlet and outlet fluid streams were less than the resolution of the temperature sensors. However, the reservoir was considered an integral part of the systems that were later tested. The conductance parameter was identified from steady-state test data for one of the test systems and is discussed in a later section.

Pump

Assuming a low overall efficiency, the thermal energy added to a system by a pump is generally small. For example, using a pump efficiency of 0.90, a flow rate of 20 gpm, and a differential pressure across the pump of 1000 psig, an estimate of the expected fluid

temperature rise is only 1.4 °F, which is below the 1.8 °F accuracy of the temperature sensing devices used in the testing program.

Most fluid power pumps have overall efficiencies greater than ninety per cent, and consequently, the temperature increase of the fluid as it passes from the inlet to the outlet port would be even less than 1.4 degrees. As a result, it was felt unnecessary to conduct steady-state or dynamic thermal tests for a hydraulic pump.

Total System Testing

Total System Without Heat Exchangers

Thermal tests on the open-center system shown in Figure 3 were conducted for constant and cyclic system loading. Operation of the system with a constant load means that the following quantities were held constant: system flow rate, differential pressure across the control valve, and the displacement of the valve spool from its center position.

In all of the system tests presented below, the mass of fluid in the system reservoir was kept the same. The importance of this is that the thermal capacitance and conductance of the system are dependent upon the mass of fluid in the reservoir. Thus, a loss of fluid means a change in the capacitance and conductance of the system, and variations of these parameters from one test to the next would have resulted in drastic changes in the models.

Cyclic loading conditions were imposed on the system by driving the valve spool with a scotch yoke mechanism sketched in Figure 10. The system flow rate was adjusted when the control valve spool was centered, and the load valve was set when the control valve spool was in an extreme

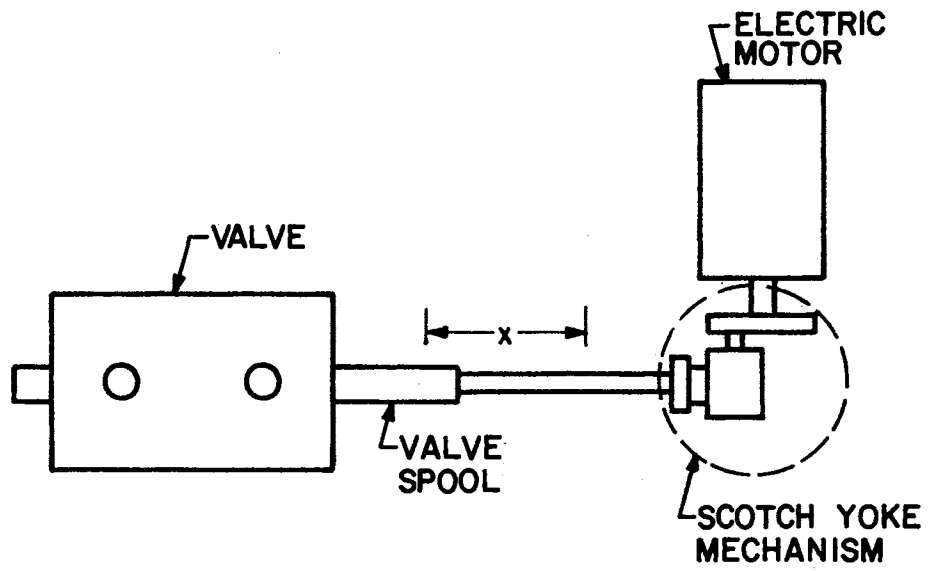


Figure 10. Scotch Yoke Mechanism

position. Tests were begun when the motor driving the scotch yoke was activated.

Temperature measurements were made at the inlet and outlet ports of the reservoir and at the inlet port to the control valve. The pump was treated as a constant heat source with an overall efficiency of ninety per cent. Heat losses from inter-connecting lines were assumed to be negligible since no measurable temperature difference existed between the control valve outlet port and the reservoir inlet port. As a result, the outlet temperature of the control valve was also the inlet temperature to the reservoir. The ambient room temperature was the reservoir ambient temperature and was recorded for all of the tests.

Steady-State Tests

Steady-state tests were run with different system flow rates, control valve spool displacements, and load pressures. Based on the data from these tests, the lumped thermal conductance parameter of the system was identified. The procedure for identifying this parameter has been discussed for the cases of liquid-to-air and liquid-to-liquid heat exchangers. Equation (39) was used to compute the numerical value of UA_R for each test. Table V summarizes these computations, and the average value of the thermal conductance of the system was 190.5 Btu/hr/°F.

In the derivation of the thermal models for this system one of the assumptions was that the thermal capacitance and the thermal conductance could be lumped into one component - the reservoir. Consequently, the value of the lumped thermal conductance obtained from these system tests can be used to verify the reservoir and the system dynamic thermal models. The difference between the two is in the inputs for each. The inlet fluid

temperature, fluid flow rate, and ambient temperature are the inputs for the reservoir, while the inputs for the system model are ambient temperature, flow rate, control valve spool displacement, and load pressure across the control valve. Only the system model is verified below, but in effect, the reservoir model is also validated with this verification.

TABLE V
SUMMARY OF STEADY-STATE TESTS FOR AN OPEN-CENTER
SYSTEM WITHOUT HEAT EXCHANGERS

Test #	Q_f	T_{fi_R}	T_{fo_R}	T_{amb_R}	UA_R
	gpm	$^{\circ}F$	$^{\circ}F$	$^{\circ}F$	Btu/hr/ $^{\circ}F$
1	7.93	131.0	118.9	86.0	148.7
2	10.04	136.9	128.7	94.1	129.7
3	12.42	143.6	138.2	93.7	300.1
4	13.74	133.8	118.4	95.0	180.2
5	13.74	139.1	119.8	95.9	193.7
Average	--	--	--	--	190.5

Dynamic Tests

A series of dynamic thermal tests were made for constant loading conditions and various flow rates, valve spool displacements, and pressure loads. Each test was run such that flow-rate, displacement,

and load pressure were kept constant at pre-selected values. The length of the tests was originally intended to be one hour; however, for some tests the temperatures being recorded exceeded 140 degrees Fahrenheit, which was the maximum range of the recorder. As a result, some of the tests were terminated before steady-state conditions were reached.

The results from test number 1 of Table VI were used to identify the lumped equivalent thermal capacitance parameter in a manner similar to that used for identifying the capacitances for the component models. The value that was obtained for C_{eq_R} was 69.42 Btu/ $^{\circ}$ F, which when combined with UA_R gave the time constant of the system as 21.86 minutes.

Knowing the capacitance and conductance parameters and the initial condition of ΔT_R , Equations (42), (43), and (44) were solved simultaneously to obtain the predicted inlet and outlet reservoir temperatures. A modified version of the open-center system program presented in Reference (16) was used to compute the rate of addition of thermal energy to the system. A flow chart of the modified program is given in Figure 11. The inputs to the program were system flow rate, spool displacement, and load pressure across the control valve. Knowing the values of UA_R , C_{eq_R} , and ΣHg , Equations (42), (43), and (45) were used to compute the inlet and outlet reservoir temperatures.

Figure 12 shows a comparison of experimental data and analytical predictions for one of the dynamic tests, and Table VI gives an error summary between experimental results and computed values for several tests. From the results shown in the figure and the error summary of Table VI, it is concluded that the dynamic model developed in Chapter IV is valid.

The same system was subjected to cyclic loading conditions created

TABLE VI

ERROR SUMMARY OF SIMULATIONS FOR OPEN-CENTER SYSTEM WITHOUT HEAT EXCHANGERS

Test #	ΔT_R			T_{fiR}			T_{foR}		
	Average % Error	Maximum % Error	Final % Error	Average % Error	Maximum % Error	Final % Error	Average % Error	Maximum % Error	Final % Error
1	1.89	7.06	0.00	0.73	1.69	0.36	0.61	1.67	0.38
2	2.60	6.67	1.12	0.76	1.70	1.70	1.47	2.47	2.47
3	2.81	11.24	1.72	0.92	1.97	1.97	2.23	4.37	2.21

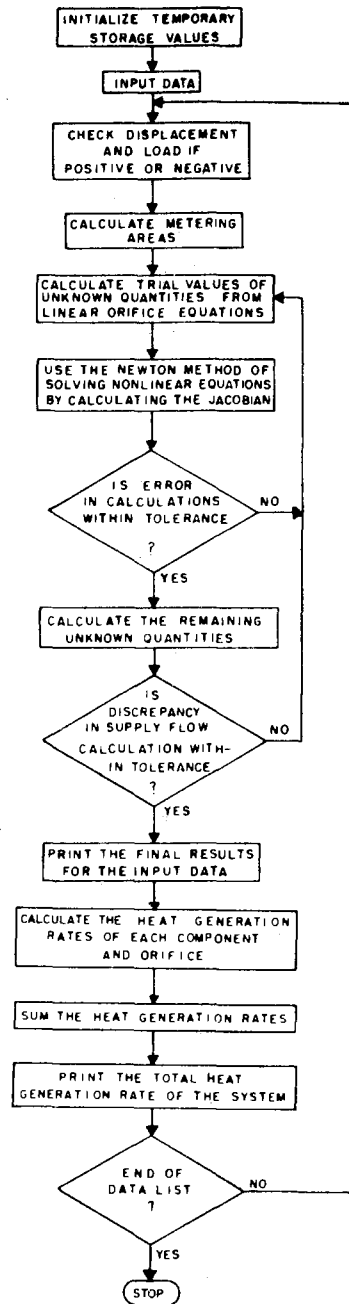


Figure 11. Flow Chart for Thermal Analysis of an Open-Center System Without Heat Exchangers

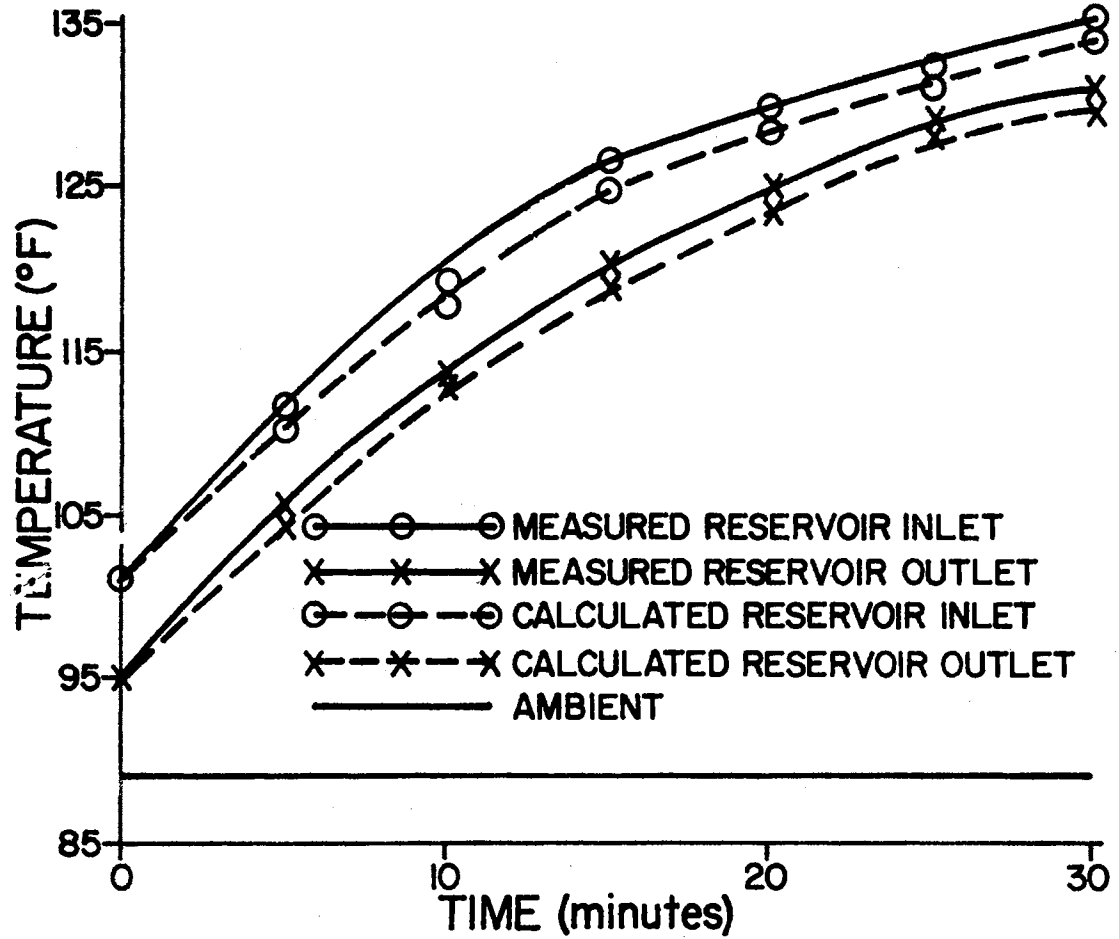


Figure 12. Test Results Versus Computed Values for an Open-System Without Heat Exchangers

by driving the control valve spool with the scotch yoke mechanism sketched in Figure 10. The valve spool displacement, system pressure, and the pressure at the working ports of the valve all varied in a periodic fashion as shown in Figure 13 for a constant pump flow rate of 13.2 gallons per minute. Experimental results for these loading conditions and flow rate are given in Figure 14. A comparison of these results with those for a constant system load and the same flow rate indicated that higher fluid temperatures occurred for the constant load rather than the duty cycle load. The results of a constant load test with a flow rate of 13.2 gallons per minute are given in Figure 15.

Total System With Liquid-to-Air Heat Exchanger

The schematic given in Figure 5 represents another system that was tested for constant and cyclic loading conditions. The temperature sensing elements were located at the inlet and outlet ports of the reservoir and the control valve. With the sensors located at these points, the temperatures at the inlet and outlet ports of each component were measured. The ambient temperatures of the heat exchanger and the reservoir were also measured for each test.

No steady-state tests were run for this system because previous tests for the liquid-to-air heat exchanger and the open-center system with no heat exchangers furnished values of all of the unknown lumped parameters for this system. (The components of this system were those tested previously.) The thermal capacitance and conductance for the system with the heat exchanger were dependent on the capacitances and conductances of the exchanger and the system without exchangers.

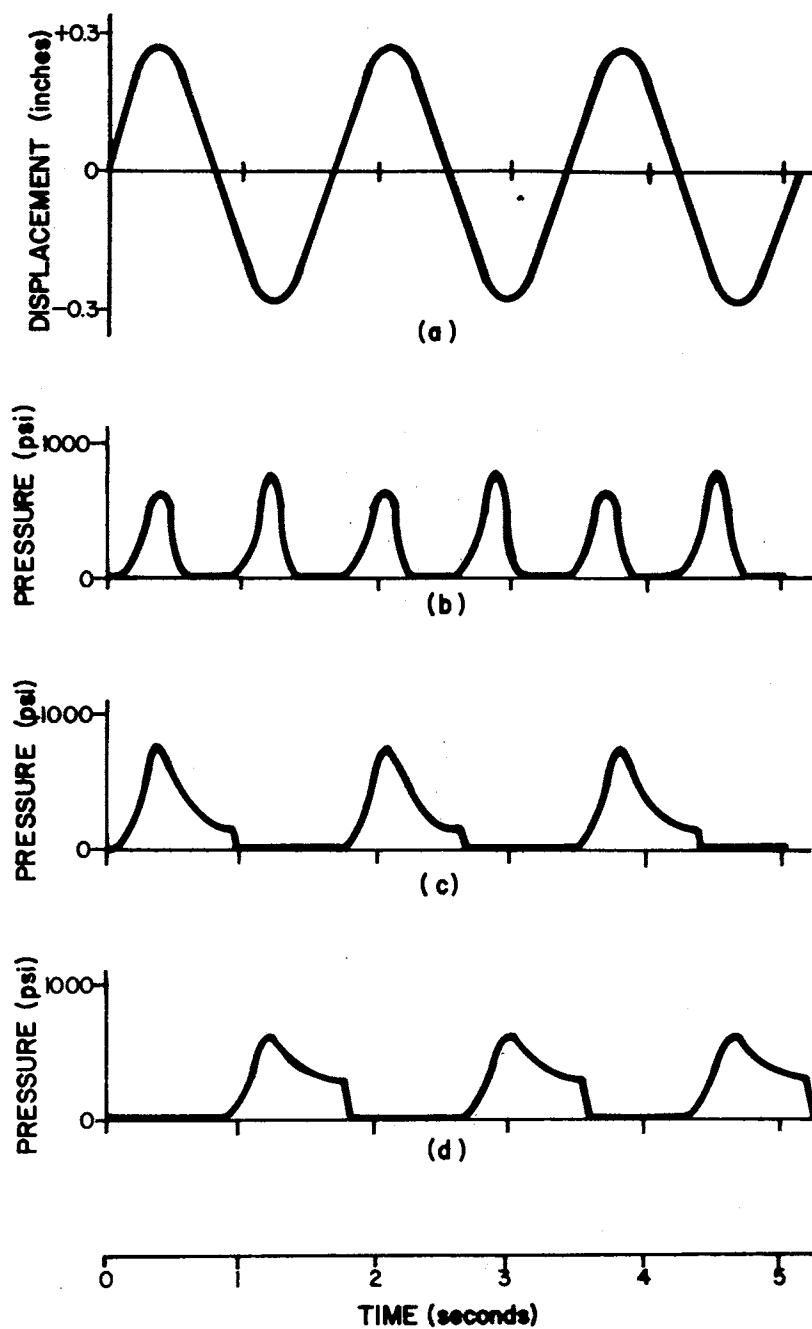


Figure 13. Cyclic Operation of an Open-Center System: (a) Spool Displacement, (b) System Pressure, (c) Pressure at Port A of Control Valve, (d) Pressure at Port B of Control Valve

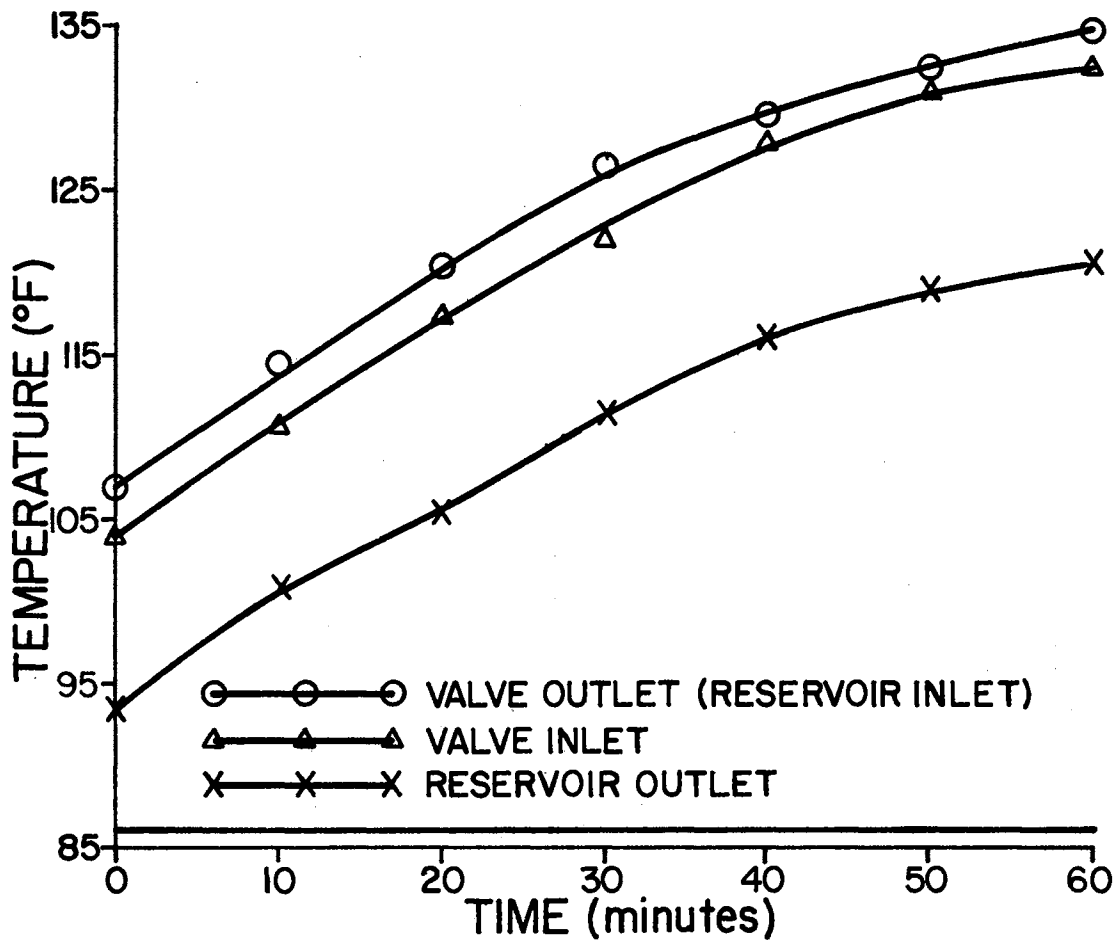


Figure 14. Test Results for Duty Cycle Operation of the System Without Heat Exchangers

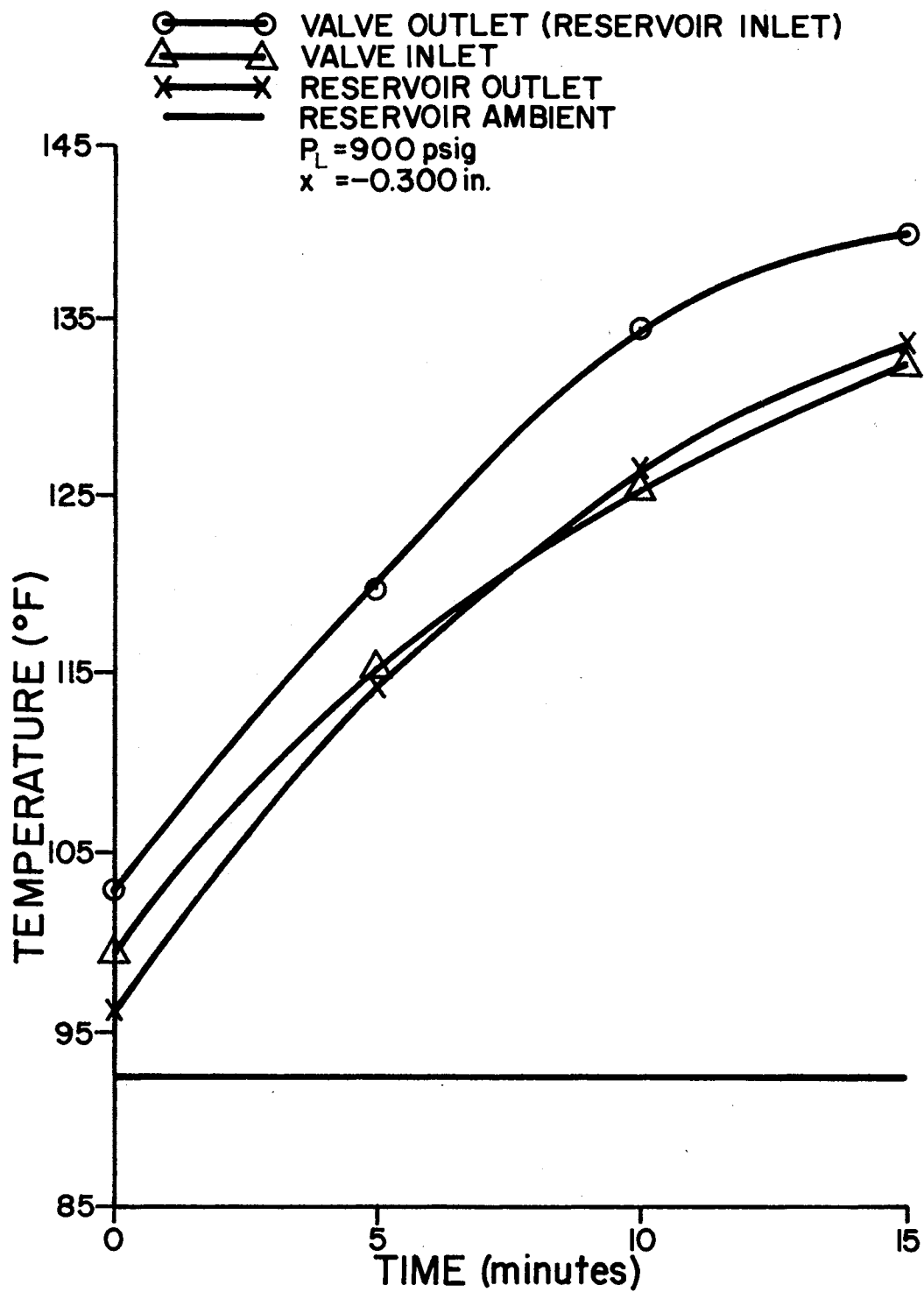


Figure 15. Test Results for a Constant System Load

Dynamic tests with constant and cyclic loading of the system were made. Only the results of the constant load tests were used to verify the model.

Dynamic Tests

Several dynamic tests with various system flow rates, loads, and constant spool displacements were made to obtain experimental data for verifying the model obtained by interfacing the component models developed earlier. The model for this system here is given by Equations (52), (53), and (54). Figure 16 shows a comparison between test data and analytical predictions of the reservoir and heat exchanger inlet and outlet temperatures for one set of test results. Table VII gives a summary of the comparison of measured temperatures with predicted temperatures. From these results, the dynamic thermal model given by Equations (52), (53), and (54) is seen to provide reasonably accurate predictions of the temperatures at different energy ports for the system.

To compare the two types of system loading conditions, results from a cyclic test (with the same flow rate as the test summarized in Figure 16) are presented in Figure 17. In testing the system without heat exchangers, it was found that a constant load produced higher temperatures than a cyclic load. Comparison of the results shown in Figure 16 and 17 also indicates this trend for the system with a liquid-to-air heat exchanger. For example, exchanger and reservoir inlet and outlet temperatures are 127.4 °F, 124.0 °F, and 122.0 °F at forty minutes for a constant load of 710 psig and -0.300 inches valve spool displacement. After forty minutes of cycling the fluid temperatures at the same points in the system are 106.3 °F, 103.6 °F, and 101.8 °F. From these results,

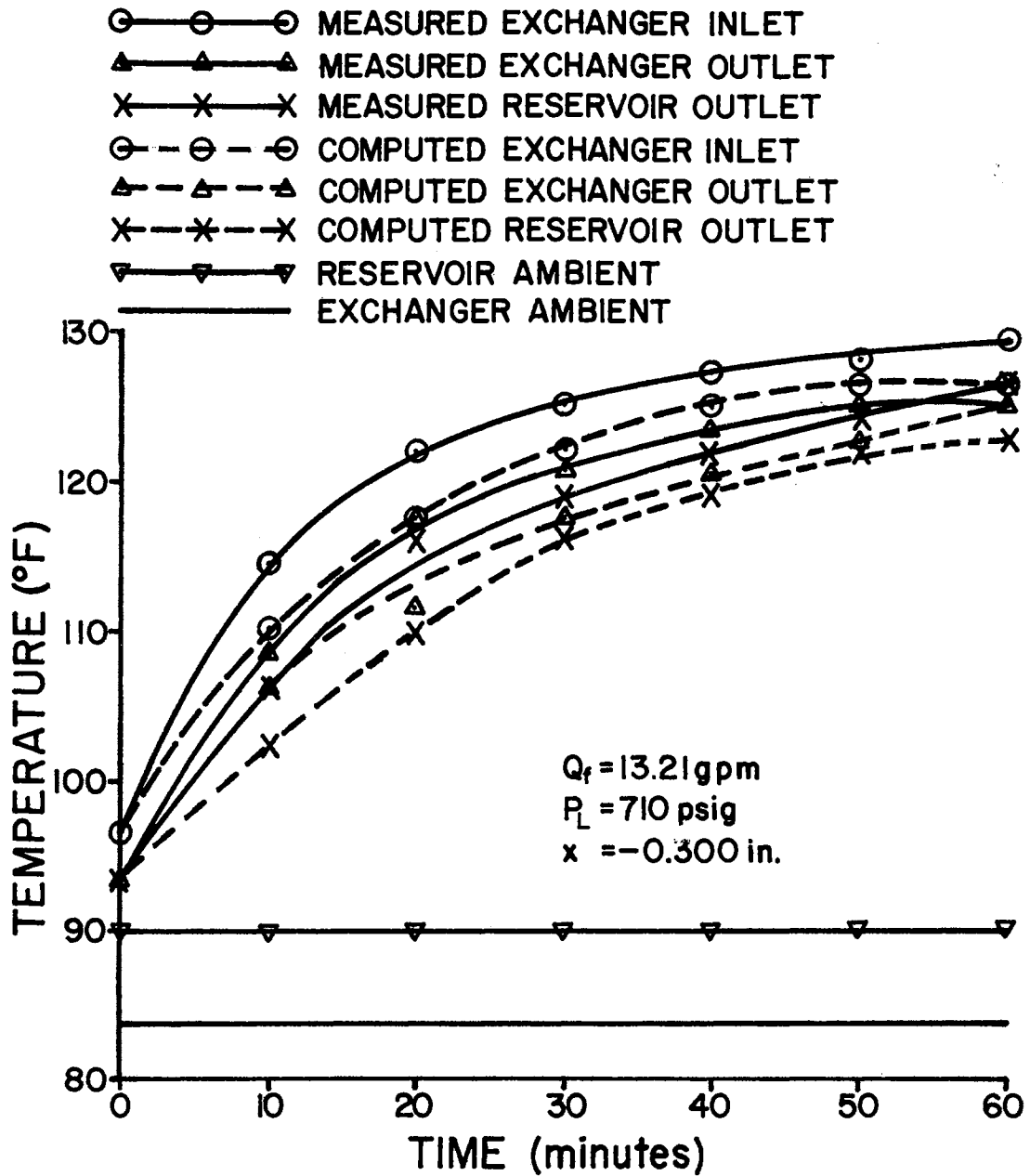


Figure 16. Test Results for an Open-Center System With a Liquid-to-Air Heat Exchanger

TABLE VII

ERROR SUMMARY FOR OPEN-CENTER SYSTEM WITH A LIQUID-TO-HEAT EXCHANGER

Test #	T_{fi_H}			T_{fo_H}			T_{fo_R}		
	Average % Error	Maximum % Error	Final % Error	Average % Error	Maximum % Error	Final % Error	Average % Error	Maximum % Error	Final % Error
1	2.49	5.94	0.03	2.47	5.70	0.22	2.94	5.07	2.59
2	1.27	2.68	0.00	0.84	1.77	1.19	3.13	5.24	2.27
3	1.82	2.76	2.76	1.60	3.17	1.29	2.99	4.19	2.95

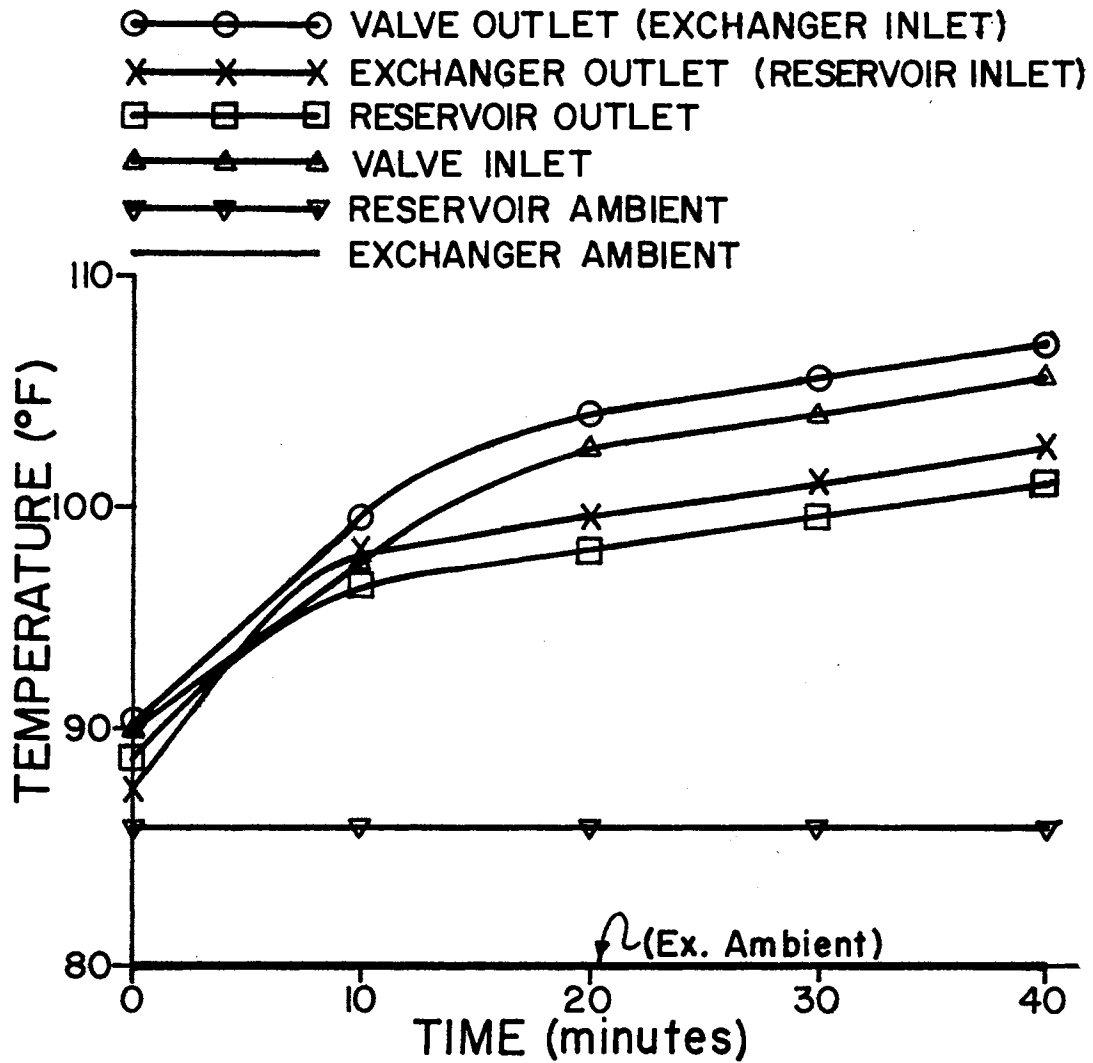


Figure 17. Cyclic Test Results for an Open-Center System
With a Liquid-to-Air Heat Exchanger ($Q_f = 50$ lpm)

it is apparent that a cyclic system load did not generate as much thermal energy as a constant system load.

In reviewing the experimental work presented in this chapter, the basic goal was to verify the various component and system lumped-parameter dynamic models that were presented in Chapters III and IV. Verification of the models demonstrates the applicability of the lumped-parameter modeling technique to thermal analysis of fluid power systems.

The importance of steady-state and dynamic test data for the identification of parameters in the dynamic models is illustrated in the cases of the liquid-to-air and liquid-to-liquid heat exchangers.

General conclusions concerning the formulation and verification of the models presented in this investigation and recommendations for further work in dynamic thermal analysis of hydraulic systems are contained in the following chapter.

CHAPTER VI

CONCLUSIONS AND RECOMMENDATIONS

Thermal modeling of hydraulic components and systems has been studied for quite some time; however, in recent years this science has come to play a more critical role than ever before. The existence of stringent duty cycles and the desires for higher power to weight ratios have necessitated better system design to ensure operation within the desired temperature ranges of the users. Heretofore, steady-state thermal analyses were considered sufficient for predicting fluid temperatures, but with the increasing demands placed on hydraulic machines such analyses no longer provide all of the information required for more effective system design. Time constants, frequency response, maximum transient temperatures, and their location in a system cannot be obtained from a steady-state thermal model. Dynamic models give this information, but prudent engineering judgment must be exercised in order to avoid tackling overwhelmingly complex mathematical models.

This investigation has presented lumped-parameter modeling techniques, which when used with basic laws of heat transfer and thermodynamics, form a suitable basis for steady-state and dynamic thermal modeling of fluid power components and systems. The low-order dynamic models that result from the application of this technique are attractive in that rapid temperature predictions can be made by solving the model equations (sometimes even in closed form). This approach to thermal modeling is

semi-empirical in that parameters have to be identified from experimental data. However, the effort required for the identification of the unknown component and system parameters is much less than that required by higher-ordered models. The resulting models are thus as mathematically simple as possible and can subsequently be interfaced with no additional complexities. Although the algebraic manipulation required for such interfacing of component models is extensive, it is fairly straightforward.

Steady-state tests were conducted for components and systems to identify the lumped thermal conductance for each. The results of the dynamic tests were also used to ascertain the accuracy of the various models. Expensive computer simulations were avoided by using simple, low-order models, and in many cases, both component and system models reduced to a set of linear algebraic and ordinary differential equations, which could be solved in closed form. The agreement between the experimental data and the predicted results of the models indicate the validity of lumped-parameter modeling of the thermal performance of fluid power systems.

The inconsistent variations of UA for increasing flow rates indicate that the temperature measurements were not accurate enough to provide good estimates of the lumped conductance parameters for the components and the systems that were tested. This implies that the values of C_{eq} that were obtained were also inaccurate.

The inability to obtain accurate temperature measurements in experimental work is the major limitation of the semi-empirical lumped-parameter approach presented in this thesis. This modeling technique is attractive, however, since it results in relatively simple

mathematical thermal models for components and systems and is considered to be applicable throughout the fluid power industry.

Recommendations for Further Study

During the course of this study, the components which significantly influence the thermal behavior of any system were modeled and tested. This does not imply that thermal models can now be constructed for a system made up of many different components. Before such a model could be obtained it would be necessary to divide the system into parts and selectively group the components together. Models for each grouping could then be derived and combined to form an overall system model. The basic idea of doing this has been advanced in this study and is amenable to lumped-parameter thermal modeling. An alternative approach would be to model the system as a whole, as demonstrated in the analysis of an open-center system without heat exchangers. Either model could be used.

Experimental testing of pumps and motors for verifying thermal models for each is mandatory before dynamic thermal analyses can be performed on large scale systems. The pump model presented here is a step in that direction, but instrumentation with better than one per cent accuracy must be available before commencing such a testing program.

The effects of interconnecting lines were neglected in the systems analyses performed in this thesis. The test systems were of such physical dimensions that this simplification could be made. However, large systems with long interconnecting lines will definitely have an effect on system temperatures, and these effects cannot be ignored.

Another promising area of investigation, which was noted as a motivating factor for the development of dynamic thermal models but not

pursued, is determination of the frequency responses of thermal models. Aircraft hydraulic systems in particular are of interest for such studies. The transmission of high pressure fluid through long, small diameter lines cause wide temperature fluctuations in these systems. Lumped-parameter modeling techniques are ideally suited for performing studies in this area.

SELECTED BIBLIOGRAPHY

- ✓ (1) Abiodun, A. A. "Steady State Heat Transfer Analysis of the 727'B' Hydraulic System." Renton, Washington: The Boeing Company, AD 701 407, December, 1969.
- (2) Abshire, R. W. "Technical Considerations in Designing a Hydraulic System for the SST." SAE Journal, Vol. 73 (May, 1965), pp. 57-62.
- (3) Blackburn, J. F., G. Reethof, and J. L. Shearer. Fluid Power Control. Cambridge, Mass.: Massachusetts Institute of Technology, 1960.
- (4) Boothe, W. A. "A Lumped-Parameter Technique for Predicting Analog Fluid Amplifier Dynamics." ISA Transactions, Vol. 4, No. 1 (January, 1965), pp. 84-92.
- 9 (5) Ebbesen, L. R. "Basic Approach to Developing Thermal Component Models for Fluid Power Systems." Basic Fluid Power Research Program Annual Report No. 6, Paper No. 72-SP-5. Stillwater, Oklahoma: Fluid Power Research Center, Oklahoma State University, 1972.
- 6 (6) Ebbesen, L. R. "Development of a Dynamic Thermal Model for a Fluid Power Pump." (Unpublished Research Proposal to the Advisory Committee, School of Mechanical and Aerospace Engineering, Oklahoma State University, Stillwater, Oklahoma, December, 1972.)
- 7 (7) Ebbesen, L. R. "Thermal Analysis of Fluid Power Systems." Basic Fluid Power Research Program Annual Report No. 6, Paper No. 72-SP-4. Stillwater, Oklahoma: Fluid Power Research Center, Oklahoma State University, 1972.
- (8) Ebbesen, L. R., B. Tomlinson, and H. R. Sebesta. "Instructions for Using the DYSIMP Sub-Program." (Unpublished Report, School of Mechanical and Aerospace Engineering, Oklahoma State University, Stillwater, Oklahoma, 1970.)
- (9) Finlay, I. C., and J. Smith. "Response of a Single/Two Pass Liquid-to-Liquid Heat Exchanger to Disturbances in Flow Rate." Journal of Mechanical Engineering Science, Vol. 9 (November 3, 1967), pp. 211-217.

- (10) Floersch, R. H., D. R. Hahn, and H. R. Sebesta. "Instructions for Performing Optimization and Model Fitting Using DYSIMP." (Unpublished Report, School of Mechanical and Aerospace Engineering, Oklahoma State University, Stillwater, Oklahoma, 1971.)
- (11) Giedt, W. H. Principles of Engineering Heat Transfer. Princeton, New Jersey: Van Nostrand Reinhold Company, 1957.
- (12) Gilles, G. "New Simple and Accurate Dynamic Model for Heat Exchangers." ASME Publication. New York: ASME, August 16, 1971.
- 179 (13) Hughes, C. W. "High Temperatures in Hydraulic Systems." Machine Design, Vol. 40 (December 19, 1968), pp. 134-138.
- (14) Ikeda, M., and S. Kodama. "Large-Scale Dynamical Systems: State Equations, Lipschitz Conditions, and Linearization." IEEE Transactions on Circuit Theory, Vol. CT-20, No. 3 (May, 1973), pp. 193-202.
- (15) Iyengar, S. K. R. "Large Scale Linear System Analysis." Basic Fluid Power Research Program Annual Report No. 8, Paper No. P74-22. Stillwater, Oklahoma: Fluid Power Research Center, Oklahoma State University, 1974.
- (16) Iyengar, S. K. R., and D. G. Miller. "Static Analysis of Directional Control Valves Using Analytical and Test Data." Basic Fluid Power Research Program Annual Report No. 7, Paper No. 73-SP-3. Stillwater, Oklahoma: Fluid Power Research Center, Oklahoma State University, 1973.
- 180 (17) Magnus, A. B. "Calculating Temperatures in Hydraulic Systems." Hydraulics and Pneumatics, Vol. 15 (November, 1962), pp. 69-74.
- ✓ (18) Mathakia, C. K. "Transient Thermal Analysis of Hydraulic Circuits." (Unpublished Master's Report, School of Mechanical and Aerospace Engineering, Oklahoma State University, Stillwater, Oklahoma, December, 1971.)
- 181 (19) McQuiston, F. C., and J. D. Parker. "Using Natural Cooling Effects." Machine Design, Vol. 42 (October 15, 1970), pp. 121-123.
- (20) Merritt, H. E. Hydraulic Control Systems. New York: John Wiley and Sons, Inc., 1967.
- (21) Messa, C. J., G. W. Poehlein, and A. S. Faust. "Heat Exchanger Modeling by Conservative Scalar Pulse Testing." Industrial Engineering Chemical Process Design and Development, Vol. 10 (November 4, 1971), pp. 466-472.

- (22) Morris, A. E. "Temperature Control in Hydraulic Systems." Applied Hydraulics, Vol. 20 (August, 1967), pp. TC/1-16.
- (23) Murali, B. N., L. R. Ebbesen, and H. R. Sebesta. "Optimization of Constrained Dynamic Systems Using the Sequential Unconstrained Minimization Techniques." Journal of Dynamic System Measurement and Control, Vol. 94 (December, 1972), pp. 319-322.
- (24) Norgard, J. S. "Thermodynamic Determination of Power Loss in Hydraulic Components." American Society of Mechanical Engineers Transactions, Paper No. 72-AW/RE 22 (March, 1973), pp. 2-7.
- (25) Parker, J. D., J. H. Boggs, and E. F. Blick. Introduction to Fluid Mechanics and Heat Transfer. Reading, Massachusetts: Addison-Wesley Publishing Company, Inc., 1970.
- (26) Parker, J. D., and F. C. McQuiston. "Thermal Analysis of Hydraulic Systems - Part I and II." Hydraulics and Pneumatics, Vol. 17 (August, 1964), pp. 57-61.
- (27) Parker, J. D., and F. C. McQuiston. "Thermal Design of Hydraulic Circuits." Stillwater, Oklahoma: School of Mechanical and Aerospace Engineering, Oklahoma State University, 1963.
- (28) Stermole, F. J., and M. A. Larsen. "Dynamic Response of Heat Exchangers to Flow Rate Changes." I & EC Fundamentals, Vol. 2, No. 1 (February, 1963), pp. 62-67.
- (29) Stern, H. "Measuring Performance of Hydraulic Machines." Product Engineering, Vol. 25 (November, 1955), pp. 150-155.
- (30) Thal-Larsen, H., and W. W. Loscutoff. "Fluid-Temperature Transients in a Dual-Heat-Exchanger System." Journal of Basic Engineering, Vol. 86 (March, 1964), pp. 23-31.
- (31) Wood, C. D. "High Temperatures in Hydraulic Systems." Machine Design, Vol. 40 (December 19, 1968), pp. 205-208.
- (32) Wood, R. K., and V. A. Sastry. "Simulation Studies of a Heat Exchanger." Simulation, Vol. 18 (March, 1972), pp. 105-111.
- (33) Catalog 1266. Racine, Wisconsin: Young Radiator Company, 1966.

APPENDIX A

LARGE SCALE SYSTEM CONSIDERATION

OF A TOTAL SYSTEM MODEL

Since the liquid-to-air heat exchanger and the open-center system without heat exchangers are considered as two separate subsystems, it is possible to use a method presented by Iyengar (14) for combining the two into one large system, provided that each subsystem is linear. To use this method, the flow rate needs to be constant so that the resulting models are linear.

It will be demonstrated in the following that the system formed by the combination of the two subsystems, although having two capacitances, is not of second-order. The state variables for the large system are tentatively defined as the differential temperatures of the heat exchanger and the reservoir.

The equations constituting the mathematical model for the liquid-to-air heat exchanger subsystem are given by Equations (14 and (15), where T_{fi_H} , and T_{amb_H} , and T_{fo_H} are the inputs and outputs, respectively.

The model for the open-center subsystem is given by Equations (22), (53), and Equation (56) below.

$$\dot{\Delta T}_R = \frac{-(k_1 UA_R + 2\rho_f Q_f C_p_f)}{Ceq_R} \Delta T_R + \frac{2\rho_f Q_f C_p_f}{Ceq_R} T_{fo_H} - \frac{2\rho_f Q_f C_p_f}{Ceq_R} T_{amb_R} \quad (56)$$

The inputs and output of this system are T_{fo_H} , T_{amb_R} , and T_{fi_H} , respectively.

The total system obtained by combining the two subsystems can then be written in matrix form as noted by Iyengar (14).

$$\dot{X} = AX + BU \quad (57a)$$

$$S: \quad Y = CX + DU \quad (58b)$$

$$U = FY + GV \quad (59)$$

where:

X is the state vector for the large system,

Y is the output vector for the large system,

U is the input vector for the large system,

V is the external input vector for the large system, and

A , B , C , D , F , and G are constant, time invariant matrices.

The mathematical model of the exchanger subsystem is given by Equations (14) and (15), and the canonical form of this model is as follows:

$$\Delta T_H \iff x_{11} \quad T_{fi_H} \iff u_{11}$$

$$T_{fo_H} \iff y_{11} \quad T_{amb_H} \iff u_{12}$$

$$\dot{x}_{11} = a_{11} x_{11} + \begin{bmatrix} b_{11} & b_{12} \end{bmatrix} \begin{bmatrix} u_{11} \\ u_{12} \end{bmatrix} \quad (60a)$$

$$y_{11} = c_{11} x_{11} + \begin{bmatrix} d_{11} & d_{12} \end{bmatrix} \begin{bmatrix} u_{11} \\ u_{12} \end{bmatrix} \quad (60b)$$

where:

\iff denotes equivalence between physical variables and model variables.

$$a_{11} = \frac{(k_1 UA_H + 2\rho_f Q_f C_{p_f})}{Ceq_H} \quad b_{11} = \frac{2\rho_f Q_f C_{p_f}}{Ceq_H} \quad b_{12} = \frac{-2\rho_f Q_f C_{p_f}}{Ceq_H}$$

$$c_{11} = 2$$

$$d_{11} = -1$$

$$d_{12} = 2$$

The canonical form for the open-center system given by (20) and (64) is as follows:

$$\Delta T_R \rightleftharpoons x_{21} \quad T_{fo_{1H}} \rightleftharpoons u_{21}$$

$$T_{fo_R} \rightleftharpoons y_{21} \quad T_{amb_R} \rightleftharpoons u_{22}$$

$$\dot{x}_{21} = a_{21} x_{21} + [b_{21} \ b_{22}] \begin{bmatrix} u_{21} \\ u_{22} \end{bmatrix} \quad (61a)$$

$$y_{21} = c_{21} x_{21} + [d_{21} \ d_{22}] \begin{bmatrix} u_{21} \\ u_{22} \end{bmatrix} \quad (61b)$$

where:

$$a_{21} = \frac{-(k_1 UA_R + 2\rho_f Q_f C_{p_f})}{Ceq_R} \quad b_{21} = \frac{2\rho_f Q_f C_{p_f}}{Ceq_R} \quad b_{22} = \frac{-2\rho_f Q_f C_{p_f}}{Ceq_R}$$

$$c_{21} = 2$$

$$d_{21} = -1$$

$$d_{22} = 2$$

The external feedback and input equation given by Equation (62) is given by the following expression:

$$\begin{bmatrix} T_{fi_H} \\ T_{amb_H} \\ T_{fo_H} \\ T_{amb_R} \end{bmatrix} = \begin{bmatrix} 0 & 1 \\ 0 & 0 \\ 1 & 0 \\ 0 & 0 \end{bmatrix} \begin{bmatrix} T_{fo_H} \\ T_{fo_R} \end{bmatrix} + \begin{bmatrix} 1 & 0 & 0 \\ 0 & 1 & 0 \\ 0 & 0 & 0 \\ 0 & 0 & 1 \end{bmatrix} \begin{bmatrix} \frac{\Sigma H_g}{\rho_f Q_f C_{p_f}} \\ T_{amb_H} \\ T_{amb_R} \end{bmatrix} \quad (62)$$

where:

$$V = \begin{bmatrix} \frac{\Sigma H_g}{\rho_f Q_f C_{pf}} \\ T_{amb_H} \\ T_{amb_R} \end{bmatrix}$$

The A, B, C, D, F, and G matrices for the large system are as follows:

$$A = \begin{bmatrix} \frac{-(k_1 UA_H + 2\rho_f Q_f C_{pf})}{C_{eq_H}} & 0 \\ 0 & \frac{-(k_1 UA_R + 2\rho_f Q_f C_{pf})}{C_{eq_R}} \end{bmatrix}$$

$$B = \begin{bmatrix} \frac{2\rho_f Q_f C_{pf}}{C_{eq_H}} & \frac{-2\rho_f Q_f C_{pf}}{C_{eq_H}} & 0 & 0 \\ 0 & 0 & \frac{2\rho_f Q_f C_{pf}}{C_{eq_R}} & \frac{-2\rho_f Q_f C_{pf}}{C_{eq_R}} \end{bmatrix}$$

$$C = \begin{bmatrix} 2 & 0 \\ 0 & 2 \end{bmatrix}$$

$$D = \begin{bmatrix} -1 & 2 & 0 & 0 \\ 0 & 0 & -1 & 2 \end{bmatrix}$$

$$F = \begin{bmatrix} 0 & 1 \\ 0 & 0 \\ 1 & 0 \\ 0 & 0 \end{bmatrix}$$

$$G = \begin{bmatrix} 1 & 0 & 0 \\ 0 & 1 & 0 \\ 0 & 0 & 0 \\ 0 & 0 & 1 \end{bmatrix}$$

Ikeda and Kodama (14) have shown that X is a state vector having the same dimension as the aggregate of the subsystems if and only if:

determinant $(I - DF) \neq 0$ for all time.

Since $(I - DF)$ for this system is the following matrix:

$$(I - DF) = \begin{bmatrix} 1 & 1 \\ 1 & 1 \end{bmatrix}$$

the determinant of $(I - DF)$ is zero for all time, and the large system cannot have a second-order state vector (i.e., $\begin{bmatrix} \Delta T_H \\ \Delta T_R \end{bmatrix}$ cannot be the state vector of the large system obtained by combining the heat exchanger and open-center subsystems). This implies that the equations for the two subsystems need to be consolidated so as to obtain a first-order model for the total system.

APPENDIX B

INSTRUMENTATION

Temperature Measurement and Recording

The temperature sensors used for measuring the temperatures of interest in the experimental testing discussed in this thesis were continuous output platinum resistance sensors. A direct current voltage supply and linear resistance bridge were necessary for powering each sensor. The output of the sensors corresponded to the scale of one millivolt equals one Centigrade degree for a range of zero to one hundred degrees Centigrade. The accuracy of these instruments over this operating range of one percent of total scale, or 1.8° F. The time constants of the sensors were 2.5 seconds.

Although the temperature sensors used were not accurate enough for thermal tests of a pump, they were felt to be accurate for components which had substantial temperature differences between inlet and outlet ports. Liquid-to-liquid and some liquid-to-air heat exchangers are components which conform to this criterion, so the use of the platinum resistance sensors with such components is acceptable.

The accuracy of the sensors becomes a relative matter for temperature measurement in total system tests. That is, the accuracy of all of the sensors must be within one percent of each other according to manufacturing tolerances. Hence, the measured results, if different from

actuality, differ only by a constant value which can be determined from a calibration check of the sensor (e.g., place the sensor into an ice bath that is at a known temperature - 32^o F - and the difference of the output reading and the known temperature is the constant value needed for correcting the measured data).

Still another problem area that must be overcome for experimental thermal analysis is the capability of recording equipment for multi-channel recording and handling of low level input signals. Most temperature measuring devices give DC outputs in the zero to one hundred millivolt range with low current (less than 10 milliamps). In contrast to this, recorders capable of recording these low level signals generally have poorer signal sensitivity for their lower recording ranges. As a result, it is necessary to amplify low level signals to be able to record them with a fair degree of accuracy. However, if the signal being recorded is noisy before amplification, after amplification it is possible that the signal must be filtered before it can be recorded. Thus, a simple problem becomes a more complex one due to exotic signal conditioning between the output and recording stages of a measured phenomenon.

The experimental tests results presented in this study were obtained only after elaborate signal conditioning between the output and recording stages. The difficulties encountered here were manifold, and are briefly discussed below.

The problem involved with the recording of the tests data presented in this thesis were different from the general description given above. First of all, the multichannel recorder could record signals only in a zero to ten millivolt range, and consequently, the output sensor signals needed to be reduced instead of amplified. These low level signals

presented another problem: impedance matching. The input impedance of the recorder was not high enough, and as a result, the input voltage signal was reduced due to the load imposed on it by the recorder. To overcome this difficulty, the sensor outputs were given a one-to-one amplification to improve their voltage-current characteristics (see Figure 18). After amplification, the voltage signal was then reduced by means of a voltage dividing circuit and was finally recorded. Little or no noise was present in the sensor signals before or after amplification, and no filtration was necessary.

Flow Measurement

The instruments used for flow measurement for experimental thermal analysis can be either turbine or target type flow transducers, either of which is satisfactory. If a recording of the flow measurement is to be made, then the target type meter will perform satisfactorily.

The flow meters used to measure fluid and coolant flow rates in the experimental tests were target type flow meters. No recording of these signals were made because the flows were held constant for all of the tests.

Pressure Measurement

Measurement of constant pressures in a hydraulic system can be done with either calibrated Bourdon gages or more sophisticated piezoelectric pressure transducers. The results of the constant load tests were obtained using both types of devices. For the case of cycling pressures, the frequency response of a Bourdon gage is too slow for accurate measurements, and a permanent record cannot be made of the gage reading. Piezoelectric

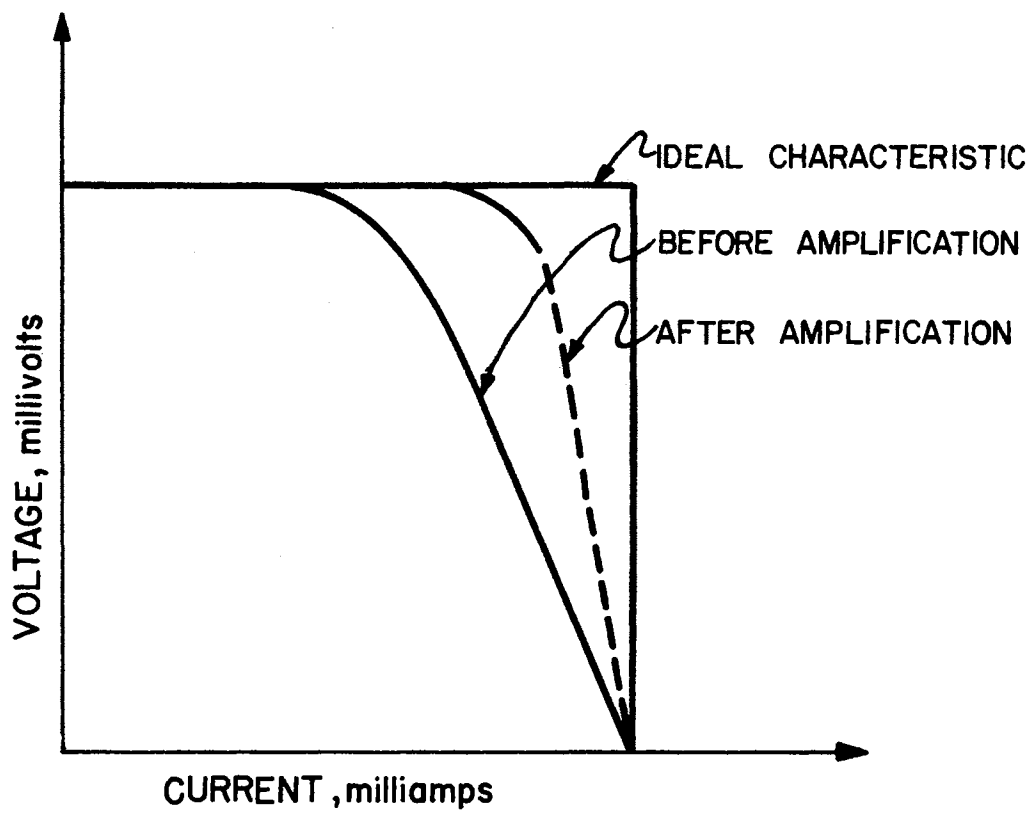


Figure 18. Voltage-Current Characteristic of Platinum Resistance Temperature Sensor

transducers are ideally suited for this application and were used to obtain the results in Figures 13 (b, c, d).

Displacement Measurement

In experimental work of any kind where directional control valves are used, it is necessary to be able to accurately measure valve spool displacement. This can be done mechanically or electronically. The mechanical elements are simple dial indicators, while the electrical devices for displacement measurement are direct current displacement transducers which give a voltage signal for a certain displacement.

A dial indicator was used to measure the valve spool displacement for the constant load tests, and a direct current displacement transducer was used to measure the valve spool displacement for the cyclic tests. Figure 13 (a) gives an example of the output of the latter.

VITA

Dennis Gary Miller

Candidate for the Degree of

Master of Science

Thesis: DEVELOPMENT AND VERIFICATION OF DYNAMIC THERMAL MODELS FOR FLUID
POWER COMPONENTS AND SYSTEMS

Major Field: Mechanical Engineering

Biographical:

Personal Data: Born in Pine Grove, Pennsylvania, January 11, 1951,
the son of Mr. and Mrs. Thomas A. Miller.

Education: Graduated from Pine Grove High School, Pine Grove,
Pennsylvania, in June, 1968; attended York College of
Pennsylvania, York, Pennsylvania, from September, 1968,
through May, 1970; received Bachelor of Science degree in
Mechanical Engineering from Oklahoma State University in 1972.

Professional Experience: Undergraduate research assistant from
January, 1972, through December, 1972, for the Basic Fluid
Power Research Program at the Fluid Power Research Center,
Oklahoma State University, studying wear in fluid power
systems; project engineer for the U. S. Army-MERDC sponsored
research concerning thermal analysis of fluid power systems
from January, 1973, through August, 1974, at the Fluid Power
Research Center, Oklahoma State University; instrument engi-
neer for Fluor Engineers and Constructors, Incorporated, 1974.